Contour current imprints and contourite drifts in the Bahamian archipelago

Mulder, Thierry; Ducassou, Emmanuelle; Hanquiez, Vincent; Principaud, Mélanie; Fauquembergue, Kelly; Tournadour, Elsa; Chabaud, Ludivine; Reijmer, John; Recouvreur, Audrey; Gillet, Hervé; Borgomano, Jean; Schmitt, Anais; Moal, Paul

published in
Sedimentology
2019

DOI (link to publisher)
10.1111/sed.12587

document version
Publisher's PDF, also known as Version of record

document license
Article 25fa Dutch Copyright Act

SEDIMENTOLOGY the journal of the International Association of Sedimentologists IAS

Sedimentology (2019) **66**, 1192–1221 doi: 10.1111/sed.12587

Contour current imprints and contourite drifts in the Bahamian archipelago

THIERRY MULDER*, EMMANUELLE DUCASSOU*, VINCENT HANQUIEZ*, MÉLANIE PRINCIPAUD*, KELLY FAUQUEMBERGUE*, ELSA TOURNADOUR*, LUDIVINE CHABAUD*, JOHN REIJMER†, AUDREY RECOUVREUR*, HERVÉ GILLET*, JEAN BORGOMANO‡, ANAIS SCHMITT* and PAUL MOAL*

**UMR 5805 EPOC, Université de Bordeaux, 33615, Pessac Cedex, France*

†College of Petroleum Engineering & Geosciences, King Fahd University of Petroleum & Minerals, Dhahran, 31261, Saudi Arabia

‡Géologie des Systèmes et Réservoirs Carbonatés Cerege, Université de Provence, 13331, Marseille Cedex 3, France

Associate Editor – Christian Betzler

ABSTRACT

New data collected along the slopes of Little and Great Bahama Bank and the abyssal plain of the Bahama Escarpment provides new insights about contour current-related erosive structures and associated deposits. The Bahamian slope shows abundant evidence of bottom current activity such as furrows, comet-like structures, sediment waves and drifts. At a seismic scale, large erosion surfaces and main periods of drift growth resulted from current acceleration related to plate tectonic processes and progressive opening and closure of gateways and long-term palaeoclimate evolution. At present-day, erosion features and contourite drifts are either related to relatively shallow currents (<1000 m water depth) or to deep currents (>2500 m water depth). It appears that the carbonate nature of the drifts does not impact the drift morphology at the resolution addressed in the present study. Classical drift morphologies defined in siliciclastic environments are found, such as mounded, plastered and separated drifts. In core, contourite sequences show a bi-gradational trend that resembles classical contourite sequences in siliciclastic deposits showing a direct relationship with a change in current velocity at the sea floor. However, in a carbonate system the peak in grain size is associated with increased winnowing rather than increased sediment supply as in siliciclastic environments. In addition, the carbonate contourite sequence is usually thinner than in siliciclastics because of lower sediment supply rates. Little Bahama Bank and Great Bahama Bank contourites contain open-ocean input and slope-derived debris from glacial episodes. Inner platform, platform edge and open ocean pelagic input characterize the classical periplatform ooze during interglacials. In all studied examples, the drift composition depends on the sea floor topography surrounding the drift location and the type of sediment supply. Carbonate particles are derived from either the slope or the platform in slope and toe of slope drifts, very deep contourites have distant siliciclastic sources of sediment supply. The recent discovery of the importance of a large downslope gravitary system along Bahamian slopes suggests frequent interactions between downslope and along-slope (contour currents) processes. The interlayering of mass flow deposits and contourites at a seismic scale or the presence of surface structures associated with both contour currents and mass flow processes shows that both processes act at the same location. Finally, contour currents have an important impact on the repartition of deep-water coral mounds. Currents can actively interact with mounds as a nutrient and oxygen supplier or have a passive interaction, with mounds solely being obstacles orienting erosion and deposition.

Keywords Bahamas, contour currents, contourites, drifts.

INTRODUCTION

Contour currents flow along continental margins at various water depths depending on their temperature and salinity, and determine erosion, transport and depositional processes involving clay, silt and fine sand. They can form erosional and depositional features from a centimetric to metric scale called ‘contourites’ (Gonthier *et al.*, 1984) and to a plurikilometric scale, so-called ‘contourite drifts’ (Stow *et al.*, 2009). Contourites were initially defined as deep-sea sediment deposited by contour currents initiated by thermohaline circulation (Heezen & Hollister, 1971). This initial and restrictive definition was extended by Stow *et al.* (2002a,b) and Rebesco (2005) to any sediment substantially reworked by bottom currents. This allowed the inclusion of deposits affected by surface currents mostly generated by wind–ocean interactions or to ancient deposits for which the hydrodynamic context is poorly known. From a general viewpoint, contour currents flow parallel to isobaths and can be considered as semi-permanent to permanent quasi-steady geostrophic flows that sunk at their equilibrium level (Rebesco *et al.*, 2008). The velocity of contour currents usually varies between 5 cm and 20 cm sec^{-1} but can be affected by surface hydrodynamic processes or by sea-floor topography and may reach velocities of up to 2·5 m sec^{-1} in particular cases when the flow section is restricted (Wynn & Masson, 2008). Topographic restrictions are mainly controlled by sea-floor morphology such as the presence of a fault wall, a ridge, a channel or a strait that can change through time (Faugères & Mulder, 2010).

The sedimentary contourite depositional sequence was initially defined in the Faro Drift (Gulf of Cadiz; Faugères *et al.*, 1984; Gonthier *et al.*, 1984). It shows a bi-gradational trend with the superposition of inverse and normal grading corresponding, respectively, to a waxing and waning current. Laminated facies are frequently interpreted as contourites, most often in fine-grained deposits (Stow, 1994) but also in sandy facies (Viana *et al.*, 1998). Shanmugam (2006, 2008) underlines the importance of sharp upper contacts and tractive structures in contour-current related deposits such as cross-bedding, lenticular, horizontal and flaser bedding. The sedimentation rate is low, and bioturbation is usually intense leading to the erasing of primary sedimentary structures (Faugères & Stow, 2008). The sediments are mainly mud, silty mud and muddy silt, and more rarely fine sand (Stow *et al.*, 2002a,b). Most of the aforementioned references deal with siliciclastic systems and literature about carbonate contour current-related systems is rare (Bein & Weiler, 1976; Cook & Mullins, 1983), with the few examples known consisting of periplatform ooze with minor clayey intervals. Most studies deal with Bahamian slopes in particular; including, the Little Bahama Bank (Mullins & Neumann, 1979; Mullins *et al.*, 1980, 1984; Austin *et al.*, 1988; Harwood & Towers, 1988; Rendle *et al.*, 2000; Rendle-Bühring & Reijmer, 2005; Lantzsch *et al.*, 2007; Mulder *et al.*, 2012b; Rankey & Doolittle, 2012; Tournadour *et al.*, 2015; Chabaud, 2016; Chabaud *et al.*, 2016), the Great Bahama Bank (Brunner, 1986; Eberli *et al.*, 1997a; Bergman, 2005; Mulder *et al.*, 2012a), the Santaren Channel (Anselmetti *et al.*, 2000; Lüdmann *et al.*, 2016; Wunsch *et al.*, 2018), the Tongue of the Ocean (Schlager & Chermak, 1979; Grammer & Ginsburg, 1992; Grammer *et al.*, 1993) and Exuma Sound (Crevello & Schlager, 1980; Austin *et al.*, 1988; Grammer *et al.*, 1999). Other examples are reported from the Maldives (Lüdmann *et al.*, 2013, 2018) and in ancient environments (Hüneke & Stow, 2008).

Current velocity controls sea floor erosion and drift construction. In addition, drift geometry is controlled by the permanency of the current activity along the sea floor, the nature of the particles carried by the current, particularly grain size, and amount of available particles (Stow *et al.*, 2008). Larger drifts can show continuous deposition over several millions of years

(Stow *et al.*, 2008). Main geometries are defined in McCave & Tucholke (1986), Stow *et al.* (1996, 2008) and Faugères *et al.* (1999), and include contourite sheeted drifts, elongate-mounded drifts, channel-related drifts and confined drifts. Rebesco *et al.* (2014) added a further three less-common drift types.

1 *Contourite sheeted drifts* are sedimentary accumulations with a moderate topography and are located on abyssal plains and in the deepest part of the basins. Sedimentation rates do not exceed 2 to 4 cm ka^{-1}. These drifts are covered with sediment wave fields and made of clayey and silty contourites consisting essentially of pelagic particles.

2 *Giant elongate-mounded drifts* are long and convex sedimentary bodies with lengths reaching tens to more than 100 km with a sedimentation rate varying from 2 to 10 cm ka^{-1} and sometimes reaching 60 cm ka^{-1}. Elongated drifts can be subdivided in plastered, detached and separated drifts. Plastered drifts are deposited by a large, low-velocity unconfined flow but flow velocity is too weak to generate erosion. They migrate parallel to isobaths but also upslope and downslope. Separated drifts form in a similar way to plastered drifts but under the action of a more energetic current. Separated and plastered drifts are usually associated depending on the flow strength. Separated drifts are bordered by depressions called moats that were defined as an erosional depression related to the presence and the intensity of a contour current on the seabed (Faugères *et al.*, 1999; Stow *et al.*, 2008). They both prograde upslope and parallel to isobaths. Detached drifts usually form at a bend of the margin and prograde downslope and perpendicular to the margin.

3 *Channel-related drifts* form in large deep-channels in which current velocity is locally increased. Contourites are thus deposited as convex, low-topography, patch drifts in the channel axis or along their sides and as contourite lobes at the channel mouth (Howe *et al.*, 1994; McCave & Carter, 1997; Reeder *et al.*, 2002).

4 *Confined drifts* form in narrow channels, gateways or gaps, and show vertical stacking of contourites with very restricted lateral migration.

5 *Localized patch drifts* with limited extension.

6 *Infill drift* usually filling a failure scar or any other topographic low.

7 *Fault-controlled drift* related to a fault scar and mixed drift related to current interaction. Recently Lüdmann *et al.* (2018) introduced a point-sourced fed, channel related, drift type named delta drift that occurred attached to the slope of a Miocene carbonate platform in the Inner Sea of the Maldives.

This paper presents a review of sedimentary evidence of contourite activity within the Bahamas region, in particular using the data obtained during recent research cruises that analyzed the Great Bahama Bank and Little Bahama Bank slopes, the southern part of Blake Plateau and the toe of the Bahama Escarpment (called Blake Escarpment when bordering the Blake Plateau or sometimes the Blake-Bahama Escarpment). The paper will only focus on the drifts for which the Carambar project added new data, i.e. the Santaren Drift, the Great Bahama Bank Drift, the Blake Plateau drifts and the imprints of deep contour currents in the western San Salvador Abyssal Plain. The review will not be extended to the Pourtales Drift, extensively studied by Bergman (2005) and the Cay Sal Bank Drift (Wunsch *et al.*, 2016) because they are the subjects of other papers in this issue (Eberli & Betzler, 2019; Paulat *et al.*, 2019). This paper will: (i) describe the sedimentary features related to bottom current activity; (ii) synthesize depositional and erosional processes by bottom currents in the Bahamian carbonate environment; and (iii) discuss contour-current–gravity flow interactions.

GEOLOGICAL SETTING AND HISTORY

At present, the Bahamian archipelago is comprised of several carbonate platforms (Fig. 1; Meyerhoff & Hatten, 1974). It extends over 1000 km and is limited westward by the Straits of Florida reaching 850 m water depth, northward by the Blake Plateau and eastward by the Blake-Bahama Escarpment, a 2000 m high submarine escarpment facing the 4000 to 5000 m Blake-Bahama Abyssal Plain. The largest platforms are Great Bahama Bank and Little Bahama Bank, which are separated by the Northwest Providence Channel. The archipelago is presently dissected by deep basins, for example Tongue of the Ocean and Exhuma Sound (TOTO and ES in Fig. 1).

The Caribbean platform probably initiated during the upper Jurassic. It formed a large platform called the 'megabank' which extended from Florida to the Blake-Bahama Escarpment in the east and the Blake Plateau in the north

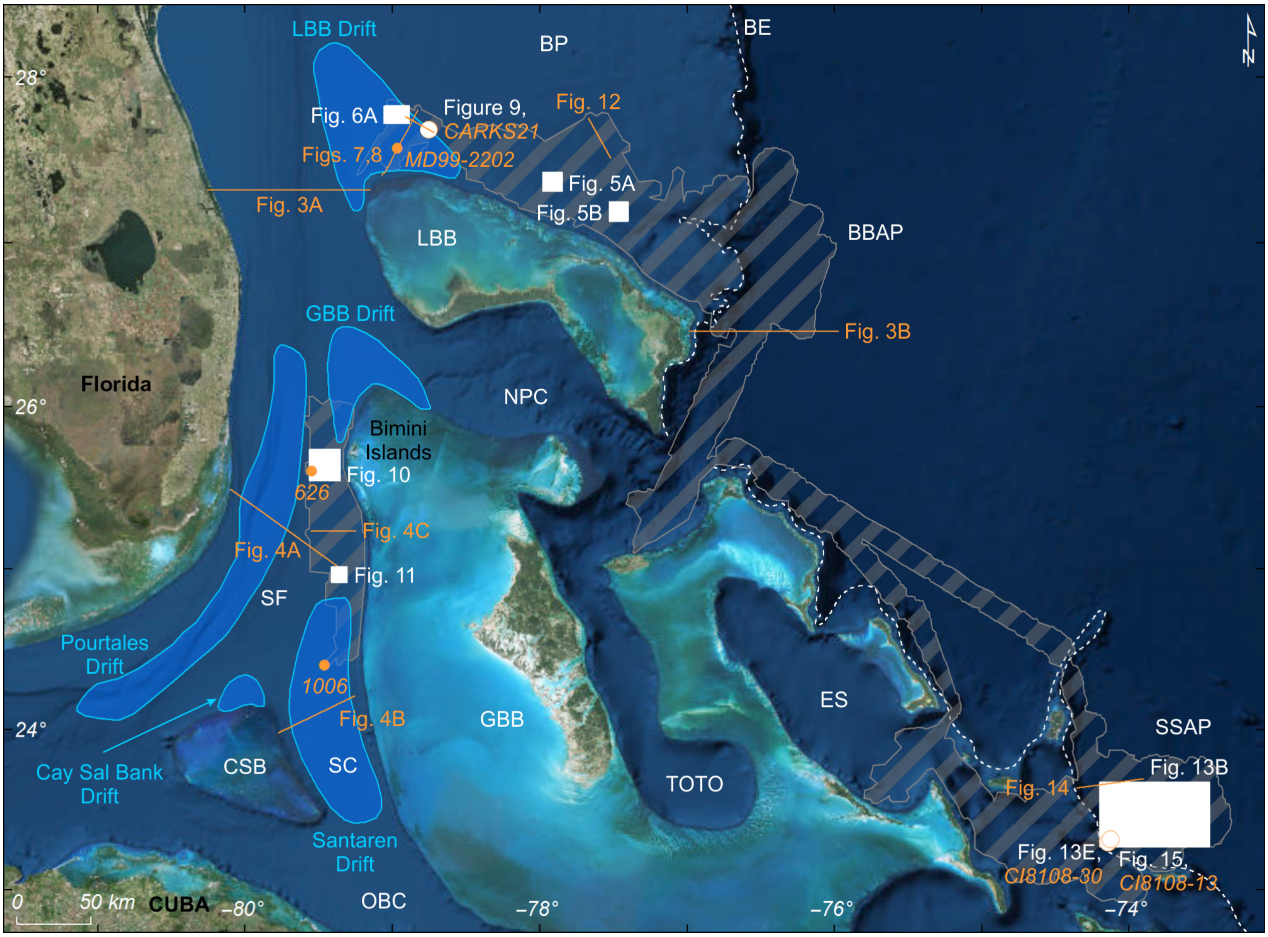

Fig. 1. Map of the distribution of the present-day active carbonate platforms, the main channels separating the platforms and the major contourite drifts along the western part of Bahamas (from Bergman, 2005; Principaud, 2015; Tournadour, 2015). BBAP, Blake-Bahamas Abyssal Plain; BE, Bahama Escarpment (white dashed line); BP, Blake Plateau; CSB, Cay Sal Bank; ES, Exuma Sound; GBB, Great Bahama Bank; LBB, Little Bahama Bank; NPC, Northwest Providence Channel; OBC, Old Bahama Channel; SC, Santaren Channel; SF, Strait of Florida; SSAP, San Salvador Abyssal Plain; TOTO, Tongue of the Ocean. The area surveyed by the Carambar cruises is shown by the striped pattern.

(Meyerhoff & Hatten, 1974; Austin *et al.*, 1988; Sheridan *et al.*, 1988). This is controversial since some studies have shown evidence of the presence of deep basins segmenting the Great Bahama Bank during the early Cretaceous (Schlager *et al.*, 1984; Sheridan *et al.*, 1988; Eberli & Ginsburg, 1989).

Since the Upper Albian, the Caribbean plate has been under a converging regime in response to subduction under the Cuba arc, and passed to a collision phase during the Palaeocene (Pindell, 1994). During the Upper Cretaceous, the ‘mega-bank’ carbonate platform was flooded, and the Bahamas formed an isolated carbonate platform (Austin *et al.*, 1988; Sheridan *et al.*, 1988). At the same time, the southern part of the Bahamas was segmented by deep north–south to WNW–ESE basins; Tongue of the Ocean, Exhuma Sound, Santaren Channel and Old Bahama Channel (OBC in Fig. 1). Convergence extended during the Middle Miocene as the Cocos plate collided with the Central American arc and the South American plate (Coates *et al.*, 2004). The Isthmus of Panama and the Central American Seaway (CAS) formed during this period, but the latter closed at *ca* 3·6 Ma (Coates *et al.*, 1992). This closure and simultaneous eustatic changes definitely led to the development of present-day thermohaline circulation (Great Conveyor Belt of Broecker, 1987) and oceanic circulation in the Atlantic Ocean was intensified (Steph *et al.*, 2006). Caribbean water salinity and temperature increased and transport towards high latitudes gradually strengthened the North Atlantic thermohaline circulation pattern. In particular, the Loop Current (LoC in Fig. 2) was initiated in the Gulf of Mexico flowing through the Straits of Florida to form the Florida Current and the northward flowing Gulf Stream (Mullins *et al.*, 1987).

PRESENT-DAY OCEANIC CIRCULATION

Oceanic circulation in the Bahamas is dominated by surface currents including the Antilles Current bathing the north of Little Bahama Bank and the Florida Current flowing between Florida and Great Bahama Bank (Figs 2 and 3A). Maximum velocity of the Antilles Current is recorded at 400 m water depth, but it is active down to 700 m water depth (Fig. 3B; Richardson *et al.*, 1969). It can reach a maximum depth of 1000 m further north along the Blake Plateau (Johns *et al.*, 1995). On the Blake Plateau and adjacent continental slopes, interaction of the deepest part of the Gulf Stream with the Deep Western Boundary Current (DWBC) can lead to substantial erosion (Pinet & Popenoe, 1985). The DWBC (formerly called Western Boundary Under Current or WBUC) represents the upper part of North Atlantic Deep Water (NADW). The Antilles and Florida currents merge north of the Straits of Florida, forming 90% of the Gulf Stream (Neumann & Pierson, 1966; Schmitz & Richardson, 1991; Evans *et al.*, 2007; Chérubin, 2014). The Florida Current is a warm salty current supplied by waters derived from the Caribbean Sea and the Gulf of Mexico (Fig. 2). A minor part is supplied by Atlantic surface waters flowing through the Old Bahama, Santaren and Providence channels (Figs 1 and 2; Leaman *et al.*, 1995). It flows northward with a surface speed ranging from 1·6 to 1·8 m sec^{-1} (South and North Florida Straight, respectively) and a velocity <20 cm sec^{-1} below 800 m water depth (Fig. 3A; Richardson *et al.*, 1969; Leaman *et al.*, 1995; Wang & Mooers, 1997). It does not appear below 1000 m water depth. The Florida Current does not fill the entire strait, and deep undercurrents and coastal countercurrents flow in opposite directions off Florida and the Bahamas with velocities of up to 0·5 m sec^{-1} on the lower slope (Grasmueck *et al.*, 2006).

The Santaren Current ('SCu' in Fig. 2) flows along the eastern part of the Santaren Channel

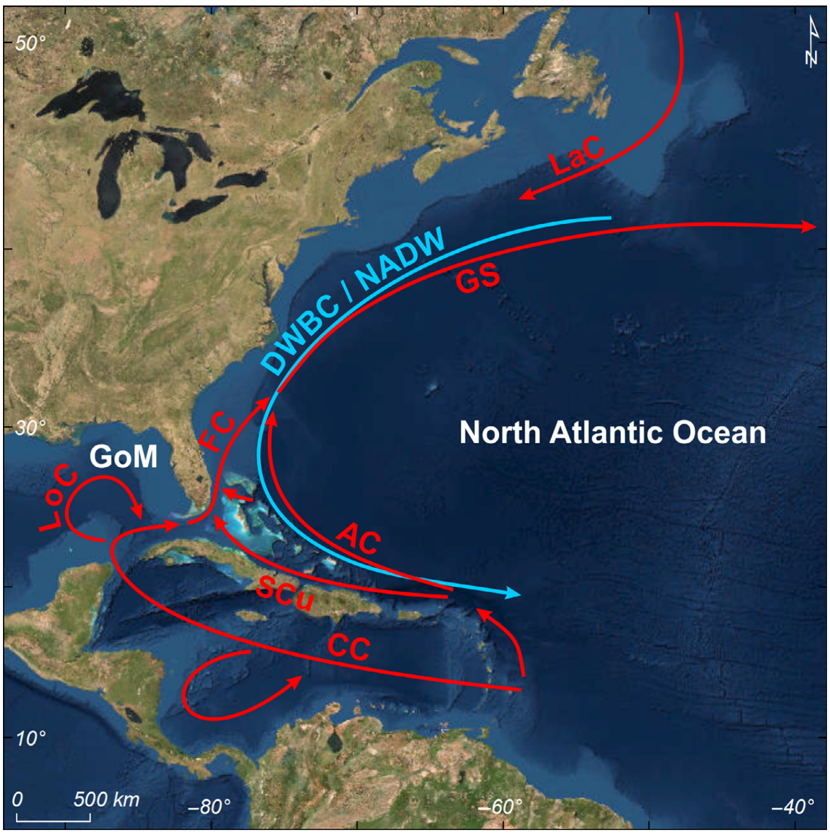

Fig. 2. Location of the Bahamian archipelago and pathway of major currents (arrows). AC, Antilles Current; CC, Caribbean Current; DWBC, Deep Western Boundary Current; FC, Florida Current; GoM, Gulf of Mexico; GS, Gulf Stream; LaC, Labrador Current; LoC, Loop Current; NADW, North Atlantic Deep Water; SCu, Santaren Current.

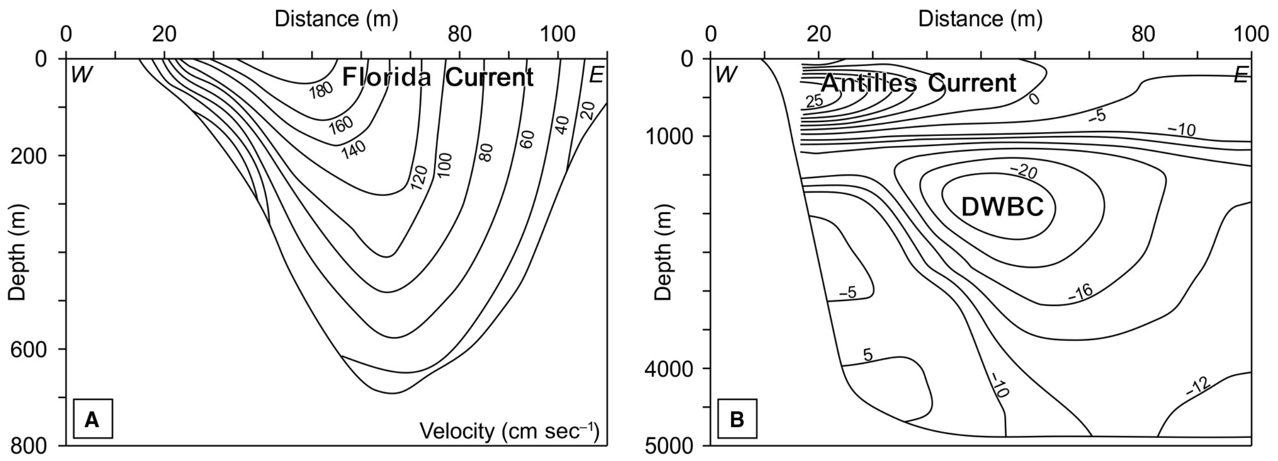

Fig. 3. Transects showing the superposed water masses (see Fig. 1 for location). (A) Florida Current (Johns *et al.*, 1995). (B) Deep Western Boundary Current (DWBC; Lee *et al.*, 1990).

with maximum velocities of 20 cm sec^{-1} at 200 to 300 m water depth (Leaman *et al.*, 1995). It enters through the Old Bahama Channel and connects subtropical north-Atlantic waters to the Florida Current (Atkinson *et al.*, 1995; Figs 1 and 2).

The Pourtales and Santaren drifts are located along Great Bahama Bank and Florida slopes, respectively, and are related to reworking of carbonate particles in the basin and at the toe of the slope by the Florida and Santaren currents (Figs 1 and 2; Table 1). These drifts have an elongate shape with lengths ranging between 200 km and 400 km, mean widths of 60 km and thicknesses varying from 600 to 1000 m (Table 1; Bergman, 2005). The Pourtales Drift (Figs 1 and 4A) was studied extensively by Bergman (2005). It is strongly asymmetrical with a well-defined moat and corresponds to an elongated detached drift according to Faugères *et al.* (1999).

The Santaren Drift is located in the axis of the Santaren Channel (Fig. 1). Other drifts surrounding the Bahamas are the Cay Sal Bank, Great Bahama and Little Bahama drifts that are located on the north-western sides of the Cal Say Bank, Great Bahama Bank and Little Bahama Bank platforms, respectively (Fig. 1). They have conical shapes extending towards north/north-west over 150 km, with widths varying between 20 km and 60 km and thicknesses ranging between 300 m and 500 m (Table 1; Mullins *et al.*, 1980; Bergman, 2005). These drifts are located on the lee side of the platforms where currents converge (Mullins *et al.*, 1980). Their internal geometry shows downlap towards the north/north-west and they are mainly supplied by off-bank transported sediments. Internal seismic facies vary from blind to laminated, medium-amplitude continuous reflectors forming a convex-up geometry thinning on the slope (Fig. 4B; Bergman, 2005). Sediment lithology is dominated by fine-grained carbonate mud (Table 1; Eberli *et al.*, 1997a,b; Rendle *et al.*, 2000). The onlap terminations of the drifts, in particular the Santaren Drift along the slopes, show interbedding of coarser sediments derived from the upper slope and laterally pinching contourite deposits (Fig. 4C). The sediment derived from the slope clearly shows a prograding trend with clear downlap geometry whilst the contourites show a retrograding trend and migrate upslope. The depression bordering the drift is partially to fully filled with the downlapping deposits.

Deep contour currents related to the thermohaline circulation also impact the Bahamas. The DWBC flows southward along the North American margin from the Irminger Basin (Greenland) and merges with the NADW at 35°N (Fig. 2; Amos *et al.*, 1971). The DWBC is constrained by the Blake Outer Ridge between 4600 m and 5000 m water depth Sheridan *et al.* (1983) and finally flows along the Blake-Bahama Escarpment between 1000 m and 4500 m water depth with its main core flowing at 2000 to 2500 m water depth (Fig. 3B; Lee *et al.*, 1990). The DWBC circulation influences sedimentation on the Blake and Bahama Outer Ridge as shown by the results of DSDP 76 (Ewing & Hollister, 1972; Sheridan *et al.*, 1983; Mountain & Tucholke, 1985; Tucholke & Mountain, 1986; McMaster *et al.*, 1989; Locker & Laine, 1992; Tucholke, 2002). This ridge is a giant, 600 km long, up to 100 km wide, elongated mounded

Table 1. Main characteristics of Bahamian drift cited in this paper including data from bibliography and original data. (1) ODP Site 626; (2) Austin *et al.*, 1986 (3) Bergman, 2005; (4) Neumann & Ball, 1970; (5) Eberli *et al.*, 1997b; (6) Chabaud *et al.*, 2016; (7) Droxler, 1984. DWBC, Deep Western Boundary Current.

Drift characteristics									Current features	
Drift Name	Shape	Length (km)	Width (km)	Thickness (m)	Drift type	Progradation	Water depth (m)	Lithology	Characteristics	Name
Pourtales (North)	Elongate	400 (3)	60 (3)	1000 (3)	Separated (3)	Upslope (3)	300 to 700	Fine-grained sand and mud (4)	S–N Moderate velocity	Florida
Pourtales (South)					Detached	Downslope (3)	500 to 900		S–N High velocity	Florida
Santaren (North)	Elongate	200	50	400	Separated	Upslope and downcurrent	600 to 900	Packstone and grainstone (1 and 2)	S–N High velocity	Florida and Santaren
Santaren (South)			60	600 (3)	Mounded (3)	Aggradation		Ooze to chalk with nannofossils, planktonic foraminifera and clay (5)	S–N Low to moderate velocity	Florida and Santaren
Cay Sal	Oblong	20 (3)	50 (3)	300 (3)	Detached (3)	Downslope and downcurrent	300 to 700		S–N Converging	Florida
Great Bahama Bank	Oblong	70 (3)	80 (3)	50 (3)	Detached (3)	Downslope and downcurrent	100 to 500		S–N Converging Moderate to high velocity	Florida
Little Bahama Bank	Oblong	30 (6)	50 (6)	<100 (6)	Detached	Aggradation and slight downslope and downcurrent	300 to 700	Periplatform ooze with planktonic foraminifera, coccoliths and aragonite needles (6)	S–N Converging Moderate velocity	Florida and Antilles
San Salvador	Elongate	Unknown	14	>130	Detached	Upslope and downcurrent	6000 to 6400	Clay (65%), other silicates (20%: quartz, feldspars), and carbonates (10%) (7)	High to moderate velocity	DWBC

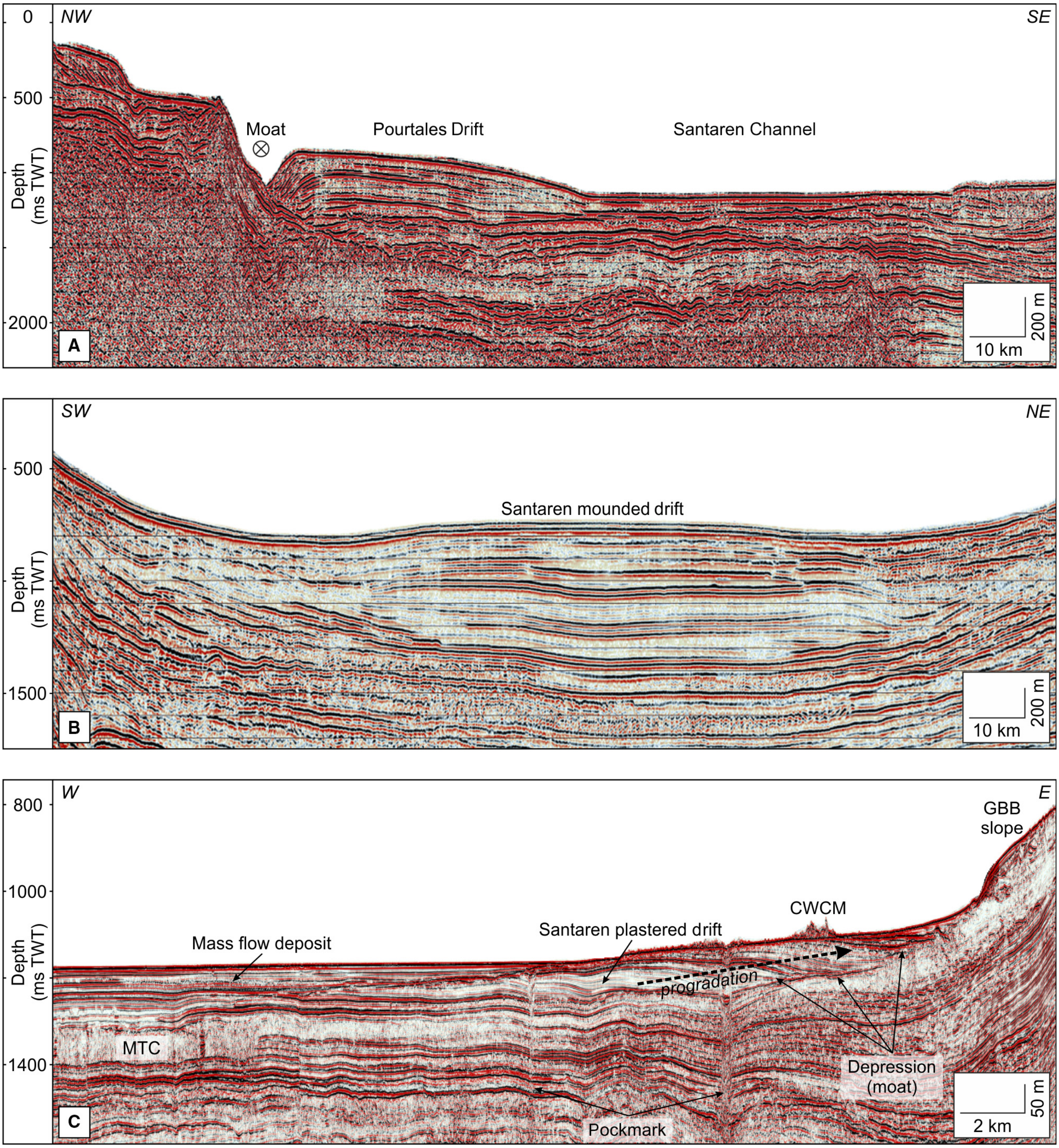

Fig. 4. (A) High-resolution seismic line through the Straits of Florida showing the geometry of the Pourtales Drift (see Fig. 1 for location; modified from Bergman, 2005). (B) High-resolution seismic line through the Santaren Channel showing the symmetrical mounded accumulation interpreted as the mounded or confined Santaren Drift (Lüdmann *et al.*, 2013; Fig. 1 for location; modified from Bergman, 2005). (C) High-resolution seismic line (Carambar cruise) along the toe of Great Bahama Bank slope showing the geometry of the Santaren Drift (from Principaud *et al.*, 2018; Fig. 1 for location). CWCM, cold water carbonate mounds; GBB, Great Bahama Bank; MTC, mass transport complex.

drift with major unconformities related to intensifications of deep-current circulation in response to global changes in deep-oceanic circulation patterns (Faugères & Stow, 2008). The 1000 to 2500 km thick ridge is partly buried but still forms a 1000 m topographic high overlying a major unconformity (noted A^u) recognized along the entire US North Atlantic margin (Tucholke & Mountain, 1979; Sheridan *et al.*, 1983; Mountain & Tucholke, 1985). The unconformity correlates with a major hiatus at Deep Sea Drilling Project Site 391 encompassing the upper Cretaceous to lower Miocene (Benson *et al.*, 1978). It corresponds to a silicified horizon which has been interpreted to have formed by an energetic sea floor current initiated at the boundary from the Eocene to Oligocene (Faugères & Stow, 2008). A second reflector (Merlin reflector), dated as late Miocene in age (12 to 10 Ma), could be correlated to a current acceleration linked with a sea-level highstand (Haq *et al.*, 1987). The unit bounded by the A^u and Merlin reflectors is marked by intense growth of the contourite. The increased sedimentation rate (19 cm ka^{-1}; Faugères & Stow, 2008) is related to an increased siliceous sediment supply provided by erosion of the Appalachian Mountains. A third unconformity is dated as late Pliocene and related to current strengthening in response to the intensified glaciation in the Arctic region and acceleration of North Atlantic Deep Water formation and contemporaneous with the closure of the Central American Seaway (Haug & Tiedemann, 1998; Reijmer *et al.*, 2002; Coates *et al.*, 2004). The late Miocene to late Pliocene period is characterized by active contourite drift growth with a sedimentation rate reaching 14 cm ka^{-1}. Above the late Pliocene unconformity, perched drifts with ages extending from Pliocene to Holocene drifts formed and consist of silty clay contourites that accumulated at a rate of 14 cm ka^{-1} (Faugères & Stow, 2008).

DATA COLLECTION AND METHODOLOGY

The Carambar cruises were operated by a scientific team lead by the University of Bordeaux and the main objective of the cruises was to better understand the sediment transfer of carbonate particles from the shallow-water platform to the adjacent basins. To date, two cruises have been completed, Carambar and Carambar 2 (Fig. 1).

The Carambar cruise was conducted between 31 October and 29 November 2010 using the *R/V Le Suroît* and analyzed the western leeward margin of Great Bahama Bank (Mulder *et al.*, 2012b), west and south of the islands of Bimini and the northern windward margin of Little Bahama Bank (Mulder *et al.*, 2012a). Onboard equipment included a Kongsberg EM302 multibeam echo sounder (bathymetry and acoustic imagery; Kongsberg Maritime, Kongsberg, Norway), a high-resolution multichannel seismic instrumentation penetrating approximately 1 sec TWT.

The Carambar 2 cruise was conducted between 30 November 2016 and 2 January 2017 with the *R/V l'Atalante* (Mulder *et al.*, 2018a,b). It investigated the eastern part of Little Bahama Bank including the Great Abaco and Little Abaco canyons (LAC; Mulder *et al.*, 2018a,b), and the Exuma Valley and Canyon as well as the San Salvador slope, down to the San Salvador Abyssal Plain. On-board equipment included a Kongsberg EM122/EM710 multibeam echo-sounder and high-resolution multichannel seismic instrumentation (four 35/35 cu in air guns and a 192-channel streamer; Kongsberg Maritime). During the two cruises, a 'Chirp' subbottom profiler (1800 to 5300 Hz frequency modulation) and a Küllenberg coring system were deployed (Kullenberg, 1947). The new data sets complement existing data of the 1981 and 1982 BACAR cruises that covered the southern part of Exuma Sound and adjacent abyssal plain (Droxler, 1984; Cartwright, 1985).

Grain-size analysis and the production of impregnated thin sections of core CARKS-21 were done at the Centre National de la Recherche Scientifique – Unité Mixte de Recherches Environnements et Paléoenvironnements Océaniques et Continentaux research laboratory of the University of Bordeaux. Grain sizes were determined using a Malvern Mastersizer S laser diffractometer (Malvern Panalytical Limited, Malvern, UK; Chabaud *et al.*, 2016).

Variations of strontium, calcium, aluminum, potassium and titanium contents were measured every centimetre in cores CARKS-21 and CI8108-13 with an Avaatech X-ray fluorescence (XRF) core scanner (Avaatech XRF Technology, Alkmaar, The Netherlands; 10 kV, 400 μA, 10 sec and 30 kV, 2000 μA, 15 sec) at the CNRS–EPOC research laboratory of the University of Bordeaux and at the Rosenstiel School of Marine and Atmospheric Sciences research laboratory of the University of Miami, respectively. Strontium counts were normalized by calcium counts in order to correct variations in water content and grain size. This ratio is used as a stratigraphical tool as an improvement on aragonite quantification described by Droxler (1984) and Croudace *et al.* (2006). The ratio [aluminum + potassium + titanium]/[calcium + strontium] is used to show the detrital influx.

RESULTS AND INTERPRETATIONS

Slope of Little Bahama Bank

At the northern slope of Little Bahama Bank, discontinuous furrows extend downslope to the basin floor from the canyon mouths near the platform margin. They are filled with low reflectivity sheet-like deposits (Fig. 5). In the eastern part of the Little Bahama Bank slope, the distributary furrows are dissected by high-reflectivity linear structures oriented N°300 to N°270 that are only visible on the EM302 reflectivity map (Fig. 5). They are located between 600 m and 1200 m on the western Little Bahama Bank slope (Fig. 5A) and between 1000 m and 1300 m water depth on the eastern Little Bahama Bank slope (Fig. 5B).

In the western part of Little Bahama Bank slope, mound-shaped structures are localized along the middle slope between 600 m and 800 m water depth. Although the largest mounds form coalescing structures aligned downslope, small sized mounds occurring at the toe of the slope are aligned perpendicular to the slope angle (Fig. 6A). They are partially covered with periplatform ooze forming a dissymmetrical, parabolic scour and associated deposits (Fig. 6B). The south-eastern flanks show either onlapping carbonate mud or a shallow depression (red arrows in Fig. 6A) whilst north-western flanks show large scours with the concave shape oriented in the upstream direction (blue arrows in Fig. 6A).

At the western end of Little Bahama Bank, the margin morphology shows a large sedimentary body forming an arcuate, oblong extension. Very High Resolution (VHR) seismic profiles (Figs 1 and 7A) show an alternation of blind and layered facies overlying an erosional surface, with low amplitude reflectors and numerous mound-shaped structures associated with fluid escape structures (Fig. 7B). Contorted reflections interpreted as relocated deposits are positioned below the erosional surface. High-resolution seismic profiles show that the layered facies pinches out downslope filling a large negative topographic depression corresponding to a buried erosional surface (scar in Figs 7 and 8). The upslope termination of this surface is marked by small mound-shaped structures within rounded topographic depressions (Fig. 7B). Core

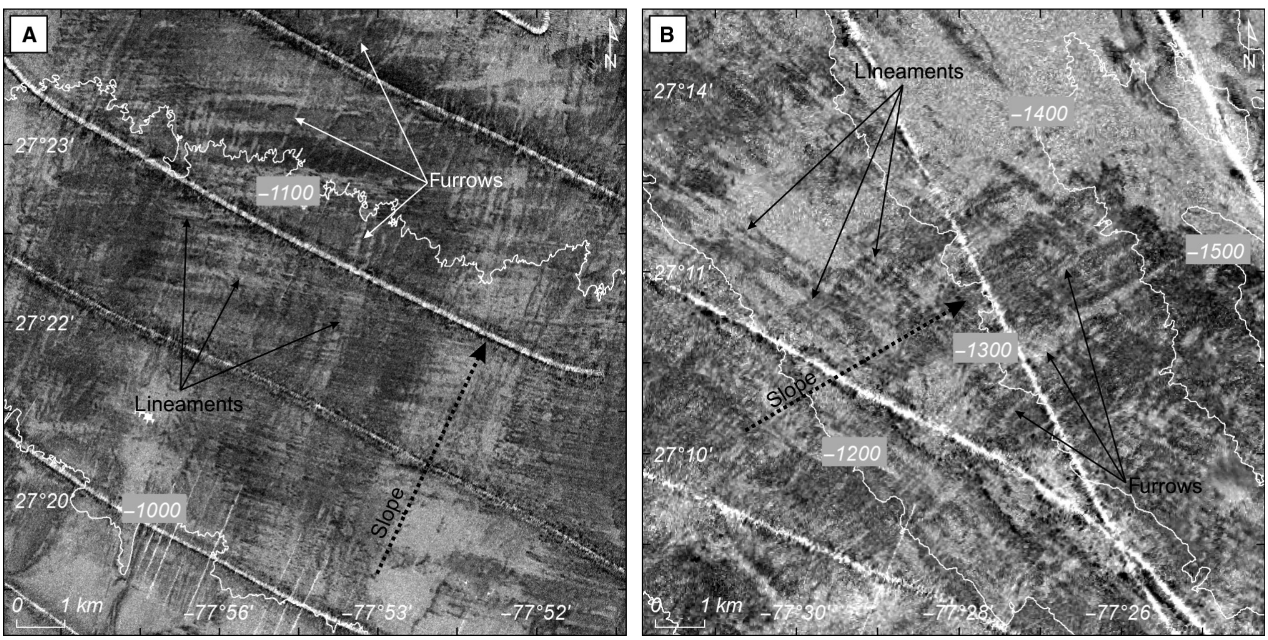

Fig. 5. Backscatter image (Carambar cruise) showing along-slope lineaments intersecting downslope furrows along Little Bahama Bank slope at: (A) western part; between 600 m and 1200 m water depth (from Tournadour, 2015); (B) eastern part between 1000 m and 1300 m water depth (see Fig. 1 for location). Clear tone indicates low backscatter.

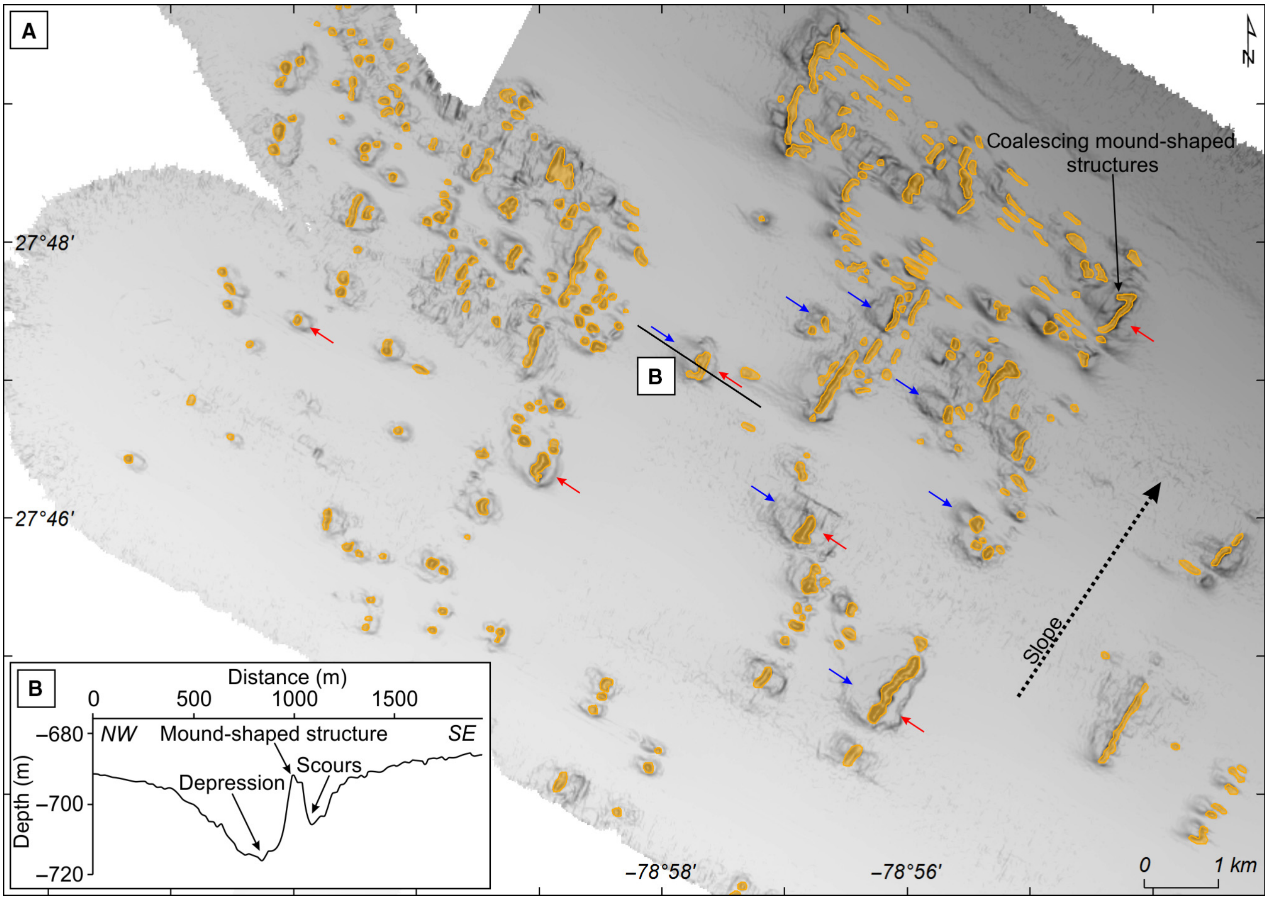

Fig. 6. (A) Bathymetric map (Carambar cruise) of mound-shaped structures in the north-western part of Little Bahama Bank showing dissymmetrical sediment accumulation; onlapping mud and topographic depression on the north-western flank (blue arrow) and scours on the south-eastern flank (red arrows). (B) Along-slope cross-section showing bathymetric changes around a mound-shaped structure. See Fig. 1 for location.

CARKS21 located at 799 m water depth just downslope from this large sedimentary body shows an alternation of fine-grained to very fine-grained, intensely bioturbated carbonate mud and thin layers of carbonate sand (Fig. 9A; Table 1). These are arranged in decimetre to several decimetre-thick bi-gradational sequences, mostly bioturbated (Fig. 9B) consisting of two superposed aragonite-enriched wackestone units separated by a grain-size peak corresponding to a partially-cemented packstone; a coarsening-up basal unit and a fining-up top unit (Fig. 9C). The packstone is enriched in pteropods and planktonic foraminifera but also in detrital particles (Fig. 9). In addition, the grain-size peak shows a positive excursion in Al + K + Si indicating an enhanced terrigenous supply.

The Sr/Ca ratio variations are perfectly correlated to marine isotopic stages (MIS) with high Sr content (aragonite) during interglacials and a decrease in Sr during glacials generating higher proportions of calcite (Fig. 9A; Droxler, 1984). In core CARKS21, the bi-gradational sequences are preferentially recorded during glacial stages (for example, MIS 2 to MIS 4, MIS 6 and MIS 8).

Slope of Great Bahama Bank

The Great Bahama Bank slope to basin area is located between N25°30/N25°50 and W79°35/W79°20, showing a large and slightly sinuous channel that extends about 20 km to the north (Figs 1, 10A and 10B). It is U-shaped and up to 6 km wide and 25 to 30 m deep (Fig. 10C). Multibeam imagery and backscatter clearly shows that the depression is covered by north–south lineaments with forming depressions a few metres deep and a few tens of metres wide (Fig. 10D). High-resolution seismic lines show that a 100 m thick, stratified sedimentary

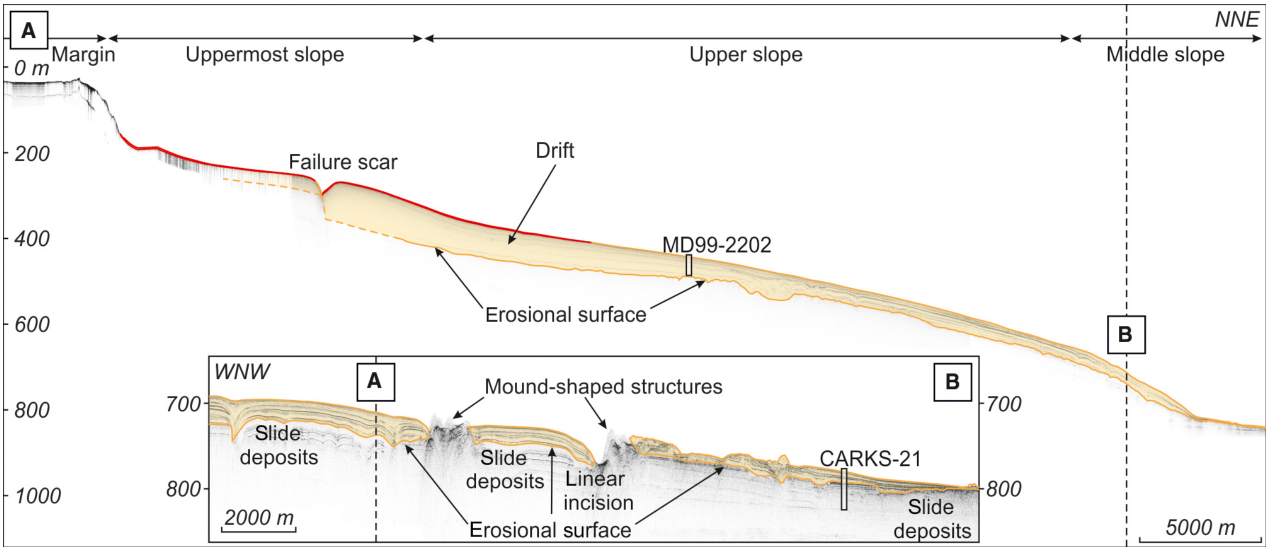

Fig. 7. Very-high resolution seismic profiles (Carambar cruise) through the recent sedimentary body forming the western corner of the Little Bahama Bank and interpreted as a periplatform drift. (A) Downdip profile. (B) Strike profile. Dashed lines indicate the location where profiles cross one another. See Fig. 1 for location.

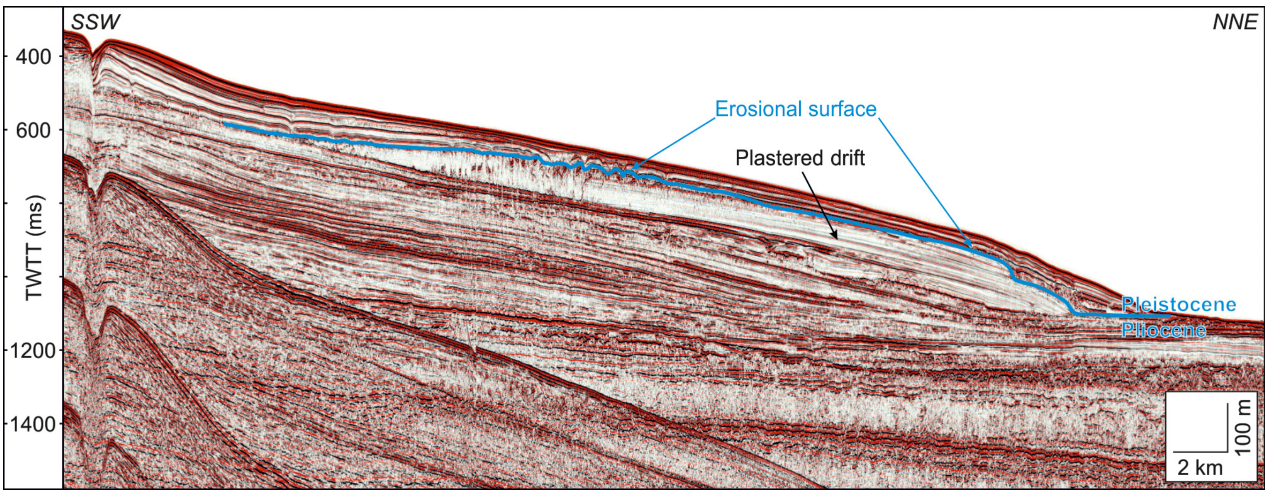

Fig. 8. Longitudinal high-resolution downdip seismic profile through the Little Bahama Bank drift filling a large mass transport complex scar (Tournadour *et al.*, 2015). See Fig. 1 for location.

structure with sub-parallel, low-amplitude reflections borders the channel (Fig. 10C). The shape and geometry of this large sedimentary structure are different from south to north. In the south (Fig. 1), the sediment body has a convex symmetrical shape centred in the channel axis. It thins towards its flanks with a dominant aggrading trend (Fig. 4B). A topographic depression separates the mounded geometry from the Great Bahama Bank slope on the eastern side (Figs 4C and 10C). The sediment body thickens in the basin and onlaps onto the Great Bahama Bank slope (Fig. 4C). However, in the north, the mounded geometry is partly obscured by slope failure deposits and, because of this feature, the sediment accumulation becomes dissymmetrical.

The slope of Great Bahama Bank shows numerous circular to elliptical structures interpreted as a cold water carbonate mound (CWCM; Fig. 11). The mounds are usually elongated in the current direction and terminate with up to 1200 m long elongated scours with a north/north-west orientation. These are located

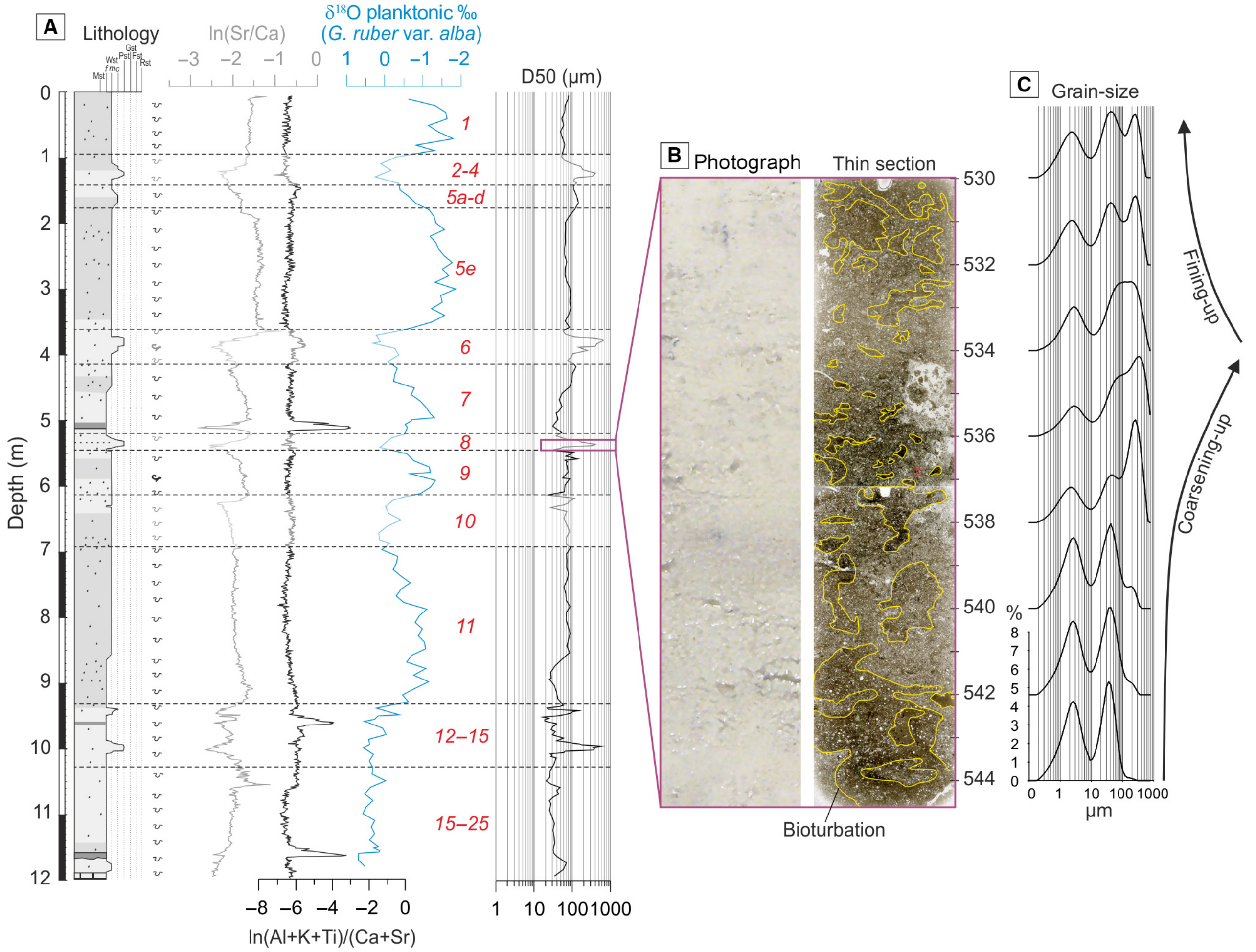

Fig. 9. (A) CARKS-21 core: Lithology, X-ray fluorescence curve for selected elements (Al + K + Ti/Ca + Sr and Sr/Ca), $\Delta^{18}O$ isotope curve with marine isotopic stages interpretation and grain-size (D50). Red numbers correspond to Marine Isotopic Stages (MIS). (B) Thin section illustrating sediment facies in core CARKS-21 (Carambar cruise) showing the superposed, intensely-bioturbated, coarsening-up and fining-up units interpreted as a contourite sequence. Yellow lines indicate the limit of bioturbation. (C) Grain-size variation along the thin section. See Figs 1 and 7B for location.

between 450 m and 850 m water depth. For most of them, the diameter varies between a few tens to a few hundreds of metres and the height from 10 to 80 m. The largest mound has a diameter of 500 m for a height of 110 m. In the northern part of Great Bahama Bank, mounds are aligned in a downslope direction (east–west) and grow on top of topographic highs (ridges) separating downslope gullies and small channels.

The backscatter also shows along-slope surface sedimentary structures across the slope of Great Bahama Bank with a large mass transport complex (MTC; Fig. 11; Principaud *et al.*, 2015). Structures are located at the top of blocks that form topographic highs along the hummocky sea floor tracing the top of mass flow deposits (Fig. 11A and B). This hummocky sea floor appears to favour bottom current-controlled depositional and erosional processes. Three types of sedimentary structures were observed; (i) south–north lineaments (50 m wide and 4 km long; Fig. 11B); (ii) scours (80 m wide, 300 m long and 5 m high; Fig. 11A); and (iii) giant crescent-marks or comet-marks (Fig. 11B) that appear on the north side of both large MTC blocks as well as CWCM that cover the sea floor in this area (Fig. 11A and C; Mullins *et al.*, 1984; Grasmueck *et al.*, 2007; Correa *et al.*, 2012a,b); they show a concave termination in the upcurrent direction.

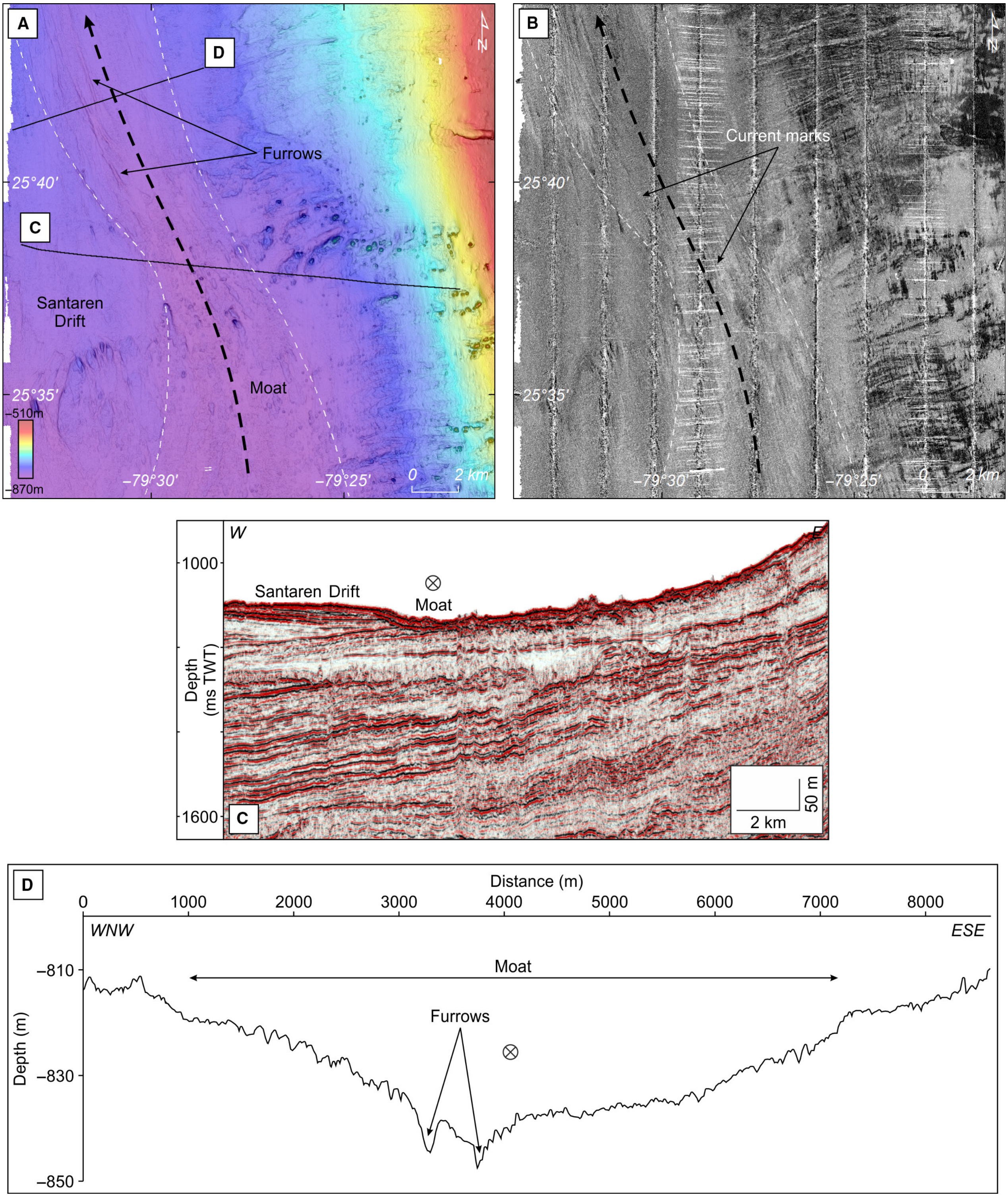

Fig. 10. (A) and (B) Bathymetric map and backscatter image (Carambar cruise) showing north–south trending, slightly sinuous channel bordering the Great Bahama Bank slope just south of Bimini Islands and interpreted as a contourite moat. (C) High-resolution multichannel seismic line showing the moat geometry. (D) Bathymetric cross-section through the moat and through furrows along the moat floor. See Fig. 1 for location.

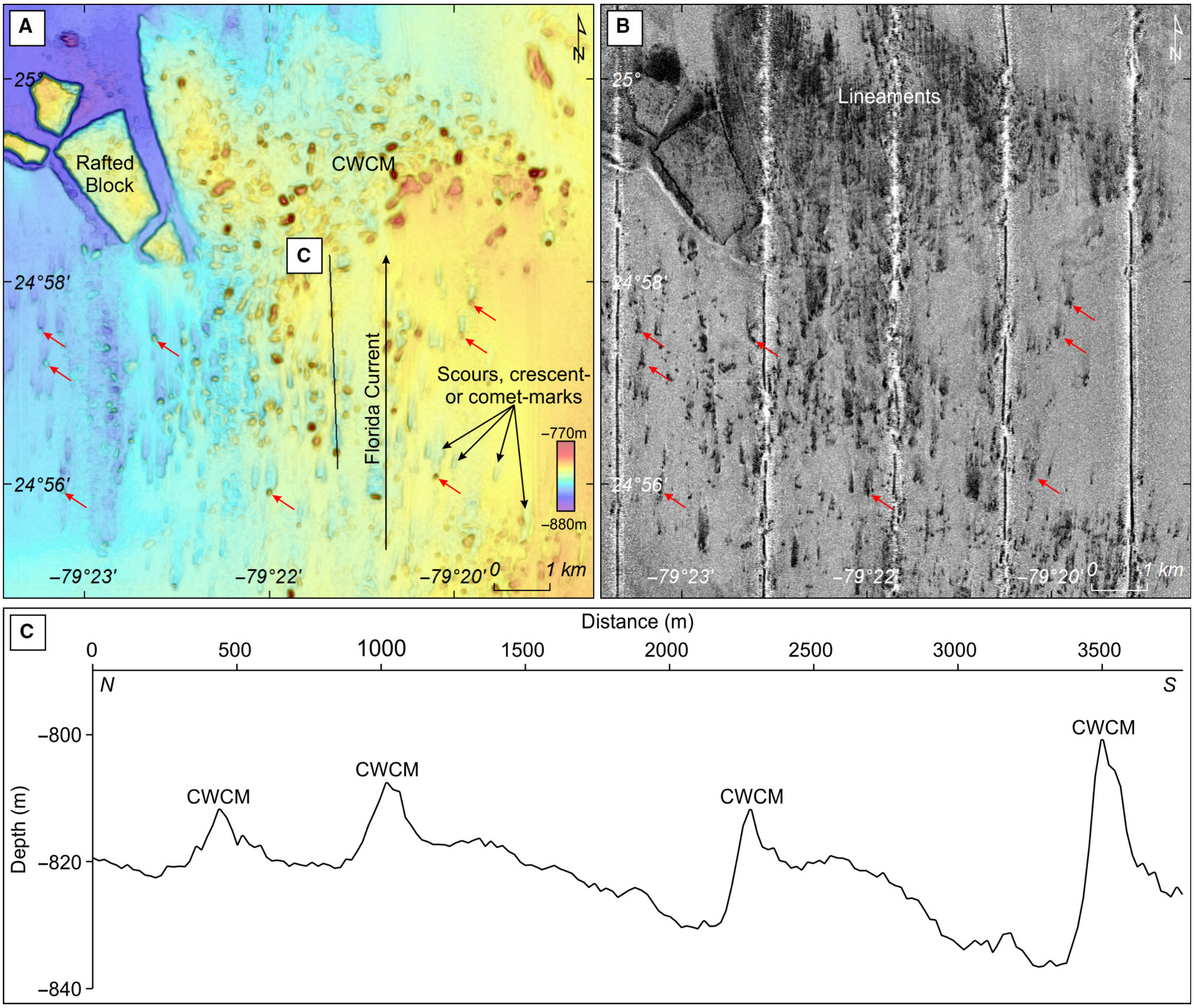

Fig. 11. (A) and (B) Bathymetric map and backscatter image (Carambar cruise) showing alignment of cold water coral mounds (CWCM) (red arrows) in the Santaren Channel in the distal part of the mass transport complex described by Principaud *et al.* (2015). (C) Cross-section through giant comet marks. See Fig. 1 for location.

Blake Plateau

The Blake Plateau is a very large plateau extending over 280 km (east–west) and 480 km (north–south) from north to south (W76°40/W79°45 and N27°45/N31°20) and a mean water depth of about 600 m ('BP' in Fig. 1). High-resolution seismic profiles show five major seismic unconformities separating six seismic units. The lowermost unconformity (green unconformity in Fig. 12) marks the top of a very flat homogeneous stratified facies with moderate amplitude parallel, mainly continuous horizontal reflections (Unit 1 in Fig. 12). Unit 2 consists of poorly stratified, low amplitude reflections. This unit appears to be largely eroded because the unconformity at the top of Unit 2 (blue unconformity in Fig. 12) locally merges with the basal unconformity. Above this unit, the seismic record enables identification of two major discontinuities separating sedimentary units (Unit 3 and Unit 4) consisting of poorly laminated, low-amplitude folded seismic facies downlapping onto the erosional surfaces. The thickest unit (Unit 3) shows parallel, discontinuous reflections that are more continuous and have stronger amplitudes upward. This unit progrades towards the NNW and is affected by undulations with

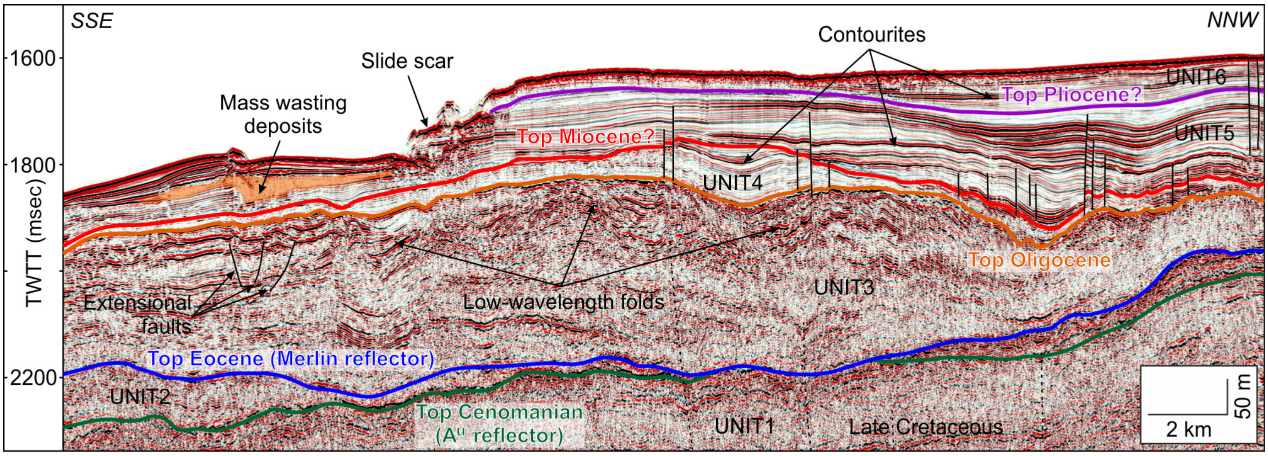

Fig. 12. High-resolution seismic line (Carambar 2 cruise) on the Blake Plateau showing the major unconformities since the late Cretaceous and related seismic units. See Fig. 1 for locations.

large wavelengths (Fig. 12). The two overlying units (Unit 5 and Unit 6) show high-amplitude parallel reflections. In Unit 6, the continuous reflector facies is laterally interrupted by transparent seismic facies. In the SSW, the deposits abruptly end at a steep submarine cliff and a chaotic seismic facies developed at the toe of this cliff.

Bahamas abyssal plain

Sedimentary structures indicative of bottom current action are also encountered in the deep part of the Bahamian sedimentary system. Multibeam bathymetry map and associated backscatter data (Fig. 13A) imaged two types of structures in waters deeper than 4500 m; (i) structures indicating a south-west/north-east flow. This includes sediment waves (sw1 and sw2 in Fig. 13B) that show an angle of 45° with regard to the axis of the Samana Channel and large-scale furrows (f1 in Fig. 13B) that radially extend from the Exuma Canyon mouth; and (ii) north–south running lineaments parallel to the Bahama Escarpment (f2 in Fig. 13B) which are interpreted as parallel, regularly spaced furrows (Fig. 13C). These furrows can reach 30 km in length and they appear quite continuous at map scale. They are 100 m wide and from 3 to 10 m deep (Fig. 13). Lineaments are associated with dissymmetrical crude sediment wave-like bedforms (sw3 in Fig. 13B) with a steep flank facing south, showing high backscatter, and a smooth flank facing north with low backscatter (Fig. 13D) indicative of a fill with low reflectivity sediment. The mean wavelength is about 500 m and the wave half-amplitude is 5 m (Fig. 13D). The furrows disappear towards the south and are replaced by sediment waves. In addition, there is a thin wedge-shape structure with a layered seismic facies lining the Blake Bahama Escarpment. It is separated from the escarpment by a small topographic depression (Fig. 14). A core from the BACAR cruise was collected in this structure but more to the south (CI8108-30; Fig. 13E; Droxler, 1984; Cartwright, 1985). Cores collected on the San Salvador Abyssal Plain (Droxler, 1984) and the related turbidite system (Cartwright, 1985) show an alternation of coarse-grained carbonated mass flow deposits and brownish silty-clays. The core shown in Fig. 15 (CI8108-13) is located on a topographic high at 4820 m water depth in the San Salvador Abyssal Plain (Droxler, 1984). The core location is interpreted as a sedimentary levée but has a more pelagic sedimentological record than other deep BACAR cores (Droxler, 1984). The XRF Sr/Ca curve shows clear alternations of sediments with low Sr/Ca values and brown clay sediments versus high Sr/Ca values with no grain-size variations (Fig. 15). This curve does not show a good correlation with δ^{18}O stratigraphy as for core CARKS21 (Fig. 9) but the isotopic curve shows that white carbonate-rich sediments are clearly correlated with interglacial stages and brown clay-rich sediments are correlated with glacial stages suggesting intensification of the terrigenous signal (Al + K + Ti; Fig. 15).

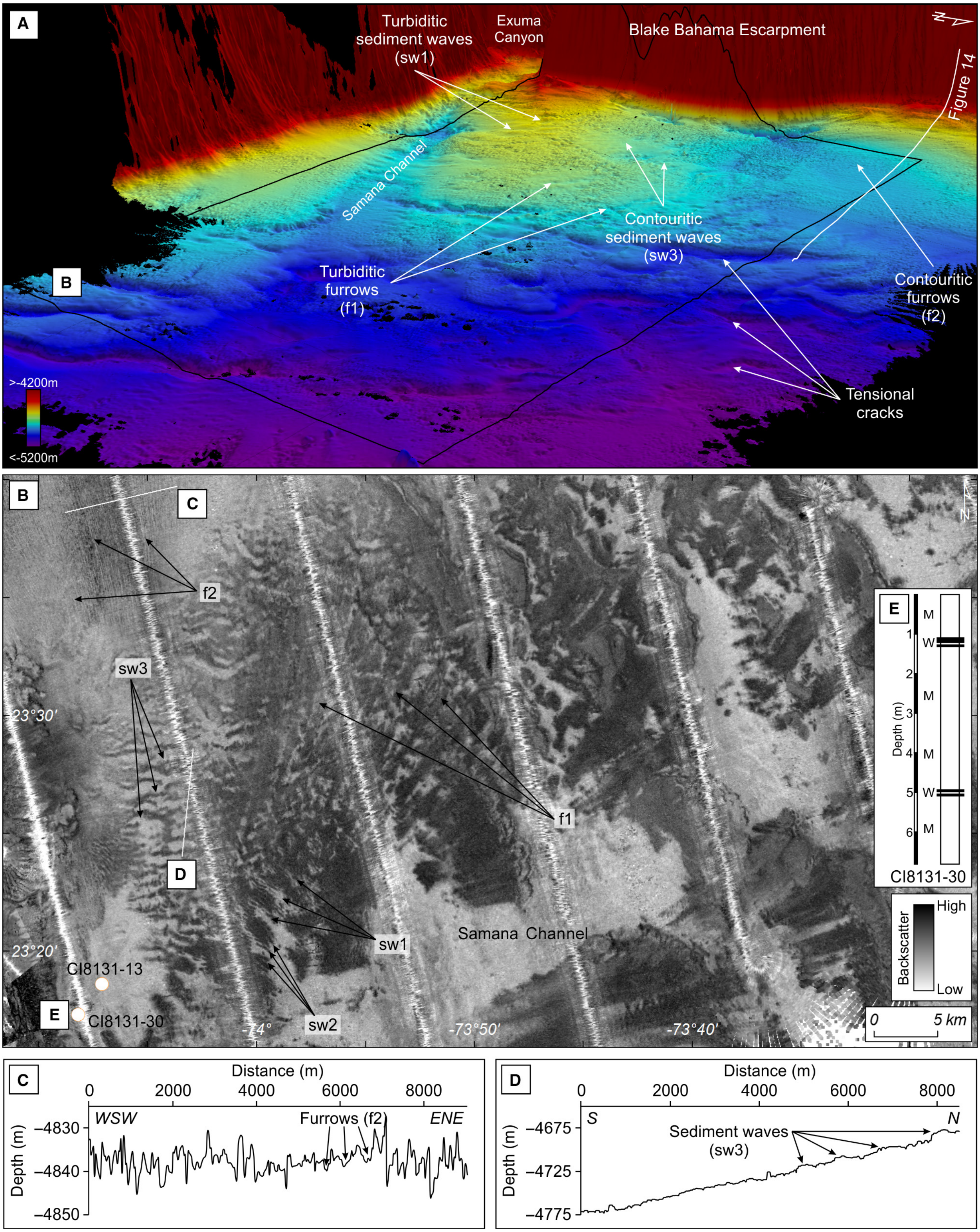

Fig. 13. (A) Multibeam bathymetry of sediment accumulation at the mouth of Exuma Canyon in the San Salvador Abyssal Plain. (B) Backscatter image of the depositional (sw1, sw2 and sw3: sediment waves) and erosive structures (f1 and f2; furrows) at the toe of the Bahama Escarpment. (C) and (D) Cross-section through the furrows and the sediment waves (Carambar 2 data). See Fig. 1 for location. (E) Core CI8131-30 showing four wackestone layers (W) interpreted as contourite peaks (redrawn from Droxler, 1984, and Cartwright, 1985). M, mudstone.

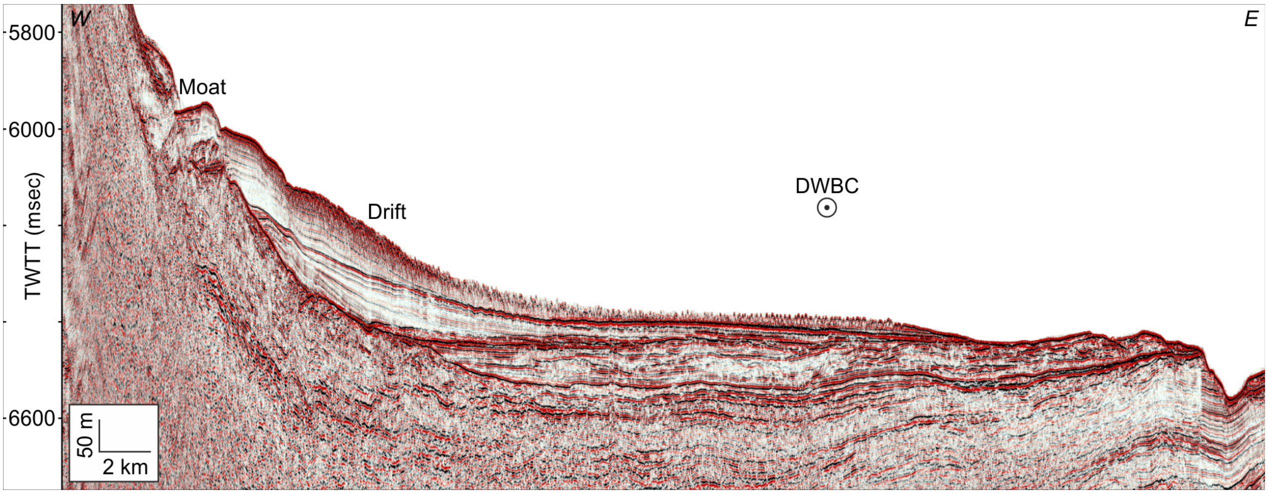

Fig. 14. High-resolution seismic line showing a small detached drift interpreted as resulting from the activity of the Deep Western Boundary Current (DWBC). See Fig. 1 for location.

DISCUSSION

Contourite sequences and contourite drifts

Little Bahama Bank

The western end of Little Bahama Bank shows a large, arcuate sedimentary body forming a sedimentary wedge downslope, filling a topographic depression (Figs 1, 7 and 8). The layered seismic facies with low amplitude reflectors is the most frequently observed seismic facies and relates to the periplatform ooze and coarse-grained sediment bed alternations collected in cores (Lantzsch *et al.*, 2007; Chabaud *et al.*, 2016). The deposits display a vertical grain-size trend with decimetre to multiple decimetre-thick sequences formed by the superposition of coarsening-up and fining-up units interpreted as contourites (Fig. 9; Gonthier *et al.*, 1984). The peak in grain-size corresponds to a packstone with wackestone at base and top. The intense bioturbation and the grain-size trend are consistent with the classical contourite sequence defined by Gonthier *et al.* (1984) and suggests overall low sedimentation rates (Chabaud, 2016; Chabaud *et al.*, 2016). The composition of the deposits varies concomitantly with variations in sea-level with coarser high magnesium calcite dominated deposits mainly occurring at the transitions from glacial to interglacial and interglacial to glacial stages, while finer intervals show higher aragonite contents and higher organic contents than the typical periplatform ooze deposits (Lantzsch *et al.*, 2007; Chabaud, 2016; Chabaud *et al.*, 2016). Chabaud *et al.* (2016) demonstrated that the overall bi-gradational grain-size trend in the carbonate contourite can be interpreted similarly to those observed in siliciclastic sequences, i.e. an acceleration followed by a deceleration of a contour current through time. The genesis of the contourite peak, however, is quite different. In siliciclastic sequences, the contourite peak corresponds to a combination of both accelerated currents along the sea floor and increased sediment supply potentially associated with increased winnowing of fine-grained particles. In the carbonate contourite sequences of Little Bahama Bank, the contourite peaks are associated with a sea-level lowstand. However, in a carbonate system, the lowstand (glacial periods) is associated with an almost complete starvation of the bank-derived particle supply because the carbonate factory on the adjacent carbonate bank is shut down. Consequently, the carbonate contourite peak corresponds to currents with enhanced velocity increasing fine particle winnowing, very low sedimentation rates (<3 cm ka^{-1}) and reorganization of the slope sediments. The overall carbonate contourite sequence is thus generally thinner (centimetres to a few decimetres thick) than the equivalent siliciclastic contourite sequence (a few decimetres to metres thick). In addition, in siliciclastic systems there are usually several contourite sequences in each glacial, each being associated with a cold episode whilst in carbonate, poor vertical resolution does not allow the distinguishing of more than one sequence during each glacial. Because of their higher porosity,

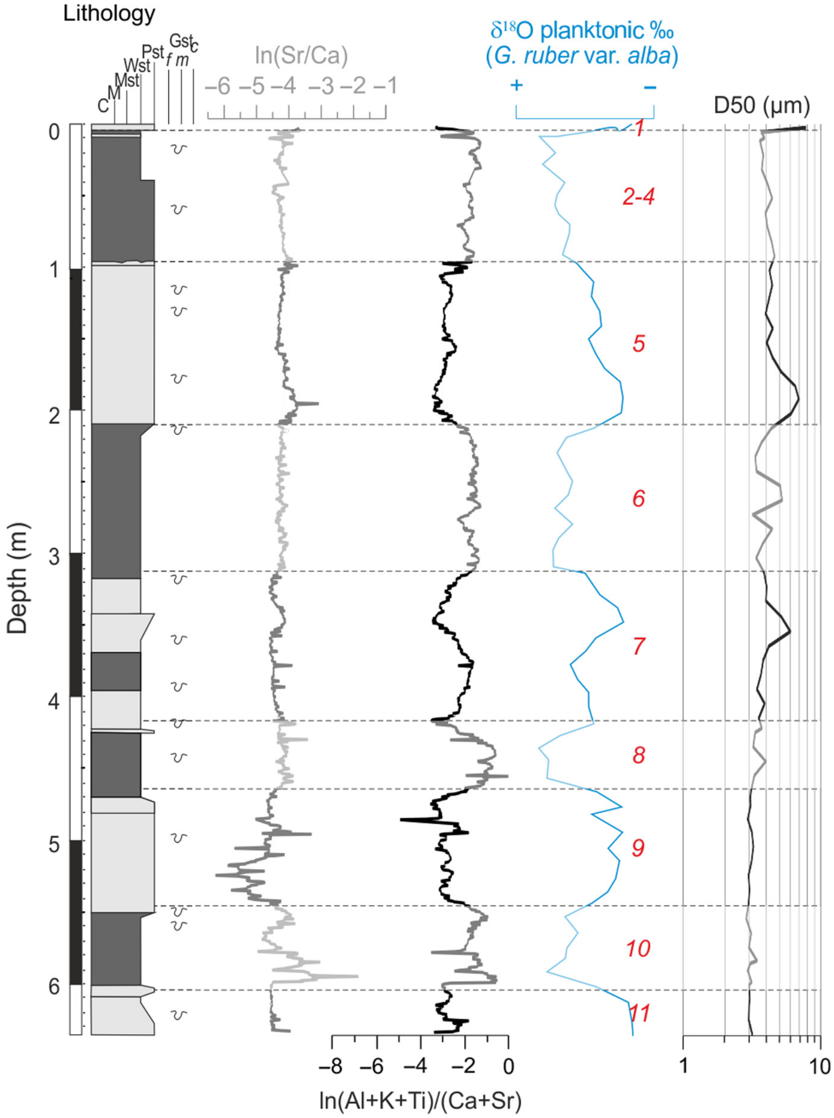

Fig. 15. Core CI8108-13 (Bacar cruise) showing the lithology, grain-size (D50) and X-ray fluorescence curves for selected elements (Al + K + Ti/Ca + Sr and Sr/Ca; from Schmitt, 2013). Note the alternation of brownish clays and white carbonated pelagic mud and the good correlation between the Sr/Ca curve and d18O isotopic curve defining glacial and interglacial stages. Red numbers correspond to Marine Isotopic Stages (MIS). See Figs 1 and 13 for location.

carbonate contourite peaks are usually partially cemented. In addition, the composition of the contourite sequence over time will depend both on the sediment source (switching on/off of the shallow carbonate factory) and on the increase or decrease of the current strength. During relative sea-level highstands [interglacial with sea-level more than −6 m present-day relative sea-level (PDRSL)], the currents interact with the off-bank sediment export from the platform and contourites are formed consisting of periplatform ooze. During these time intervals the sedimentation rate is relatively high (10 to 30 cm ka^{-1}). The Antilles Current has a low energy and flows at shallow water depth (400 m). When sea-level drops (interglacial with sea-level ranging between −6 m and −40 m PDRSL), the contourite is fed by carbonate sediment production on the marginal terraces surrounding the platform. It shows wackestone facies including aragonite mud with few planktonic organisms (Chabaud, 2016; Fauquembergue *et al.*, 2018). Grains are coarser than during highstands but sedimentation rate is low (2 to 10 cm ka^{-1}). During lowstands, sediment supply and sedimentation rates are very low. The sediments show a packstone facies enriched in planktonic foraminifera and pteropods (Chabaud, 2016), and contourites essentially form at greater water depth (600 m) following the deepening of the strong intensity Antilles Current. This is also consistent with strengthening and deepening of the Florida Current in the North Providence Channel, similar to what was observed by Brunner (1975) in the Strait of Florida. The typical intensely-bioturbated mottled facies of Gonthier *et al.* (1984) in the siliciclastic contourite facies model is very difficult to identify in a carbonate contourite because the carbonate sequence is condensed and because of very small variations in grain-size. Additionally, it was not possible to identify ichnofacies.

The large oblong sedimentary body is interpreted as a large contourite drift. Morphologically, it resembles a detached drift (Faugères *et al.*, 1999) but because it is supplied by carbonate platform-derived material it can be also classified as a periplatform drift (Betzler *et al.*, 2014). Its particular shape is related to merging of a westward flowing Antilles Current and a northward flowing Florida Current (Figs 1 and 2). The resulting current flows northward explaining why the drift is mainly aggrading with a small northward prograding trend (Figs 7 and 8). The drift fills a large depression interpreted as a failure scar that was formed by a large mass transport complex (MTC) that occurred during the late Miocene (Fig. 7; Tournadour, 2015; Tournadour *et al.*, 2015). Tournadour *et al.* (2015) suggested that the acceleration of the Antilles Current along the Little Bahama Bank slope observed during this period as marked by a large unconformity could result in increased sedimentation rates and overloading of the slope, which would represent a major preconditioning factor of the release of the MTC.

Great Bahama Bank

Along the Great Bahama Bank slope, the mounded stratified morphology prograding upslope, as shown by toe of slope onlapping reflectors, can also be interpreted as a large contourite drift (Fig. 4C). This drift (the Santaren Drift) occurs in the basin at water depth greater than 850 m and extends longitudinally from the Santaren Channel in the south to 25°N. It is about 200 km long, 50 to 60 km wide and 400 to 600 m thick from north to south (Fig. 1 and Table 1). This is consistent with the interpretation of Austin *et al.* (1986) and Schlager *et al.* (1988) who recognized Langhian contourite deposits at ODP Site 626. In the southern part, the symmetry of the deposits suggests that they form a mounded drift according to Bergman (2005) and a confined drift according to Lüdmann *et al.* (2013) and the classification of Faugères *et al.* (1999) (Fig. 4B). In the northern part, the asymmetrical geometry indicates a separated drift (Fig. 4C; Faugères *et al.*, 1999). At this location, the drift is bordered by a moat (Fig. 10A to C). The seismic line in Fig. 4C shows that a palaeomoat exists and that this separated drift is not a recent feature at this location. Cores from ODP Site 1006 document that this seismic unit consists of very fine-grained stratified aragonite-rich (up to 85%) periplatform ooze with minor high magnesium calcite, low magnesium calcite, dolomite and quartz (Table 1; Eberli *et al.*, 1997a,b; Rendle *et al.*, 2000; Rendle-Bühring & Reijmer, 2005; Principaud *et al.*, 2018).

In addition to the north to south morphological variation of the drift (Fig. 4), there is a change in the nature and texture of the sediment forming the contourites. In the southern part, contourites are dominated by carbonate muds (nannofossil ooze/chalk in ODP Site 1006; Fig. 1; Table 1; Austin *et al.*, 1986; Eberli *et al.*, 1997a,b; Rendle *et al.*, 2000; Rendle-Bühring & Reijmer, 2005). Coarser deposits including packstones and grainstones characterize the northern part (ODP Site 626; Fig. 1; Table 1; Austin *et al.*, 1986). This coarsening is interpreted as the result of the current acceleration from the Santaren Channel to the Straits of Florida. At present-day, the Florida Current seems particularly erosive along the Bimini slope (Fig. 10). This is shown by the occurrence of medium to coarse foraminiferal sand with a reduced percentage of mud-size particles beyond 800 m water depth. The north–south evolution of grain-size (coarsening northward) is consistent with drift evolution from symmetrical mounded drift to a separated drift with a clear erosional moat. Both suggest intensification of the current from south to north along Great Bahama Bank.

The drift morphology also changed over time (see also Paulat *et al.*, 2019). The morphology was flat during the Langhian and became more and more convex during the Miocene, and at the same time showed increased interbedding with slope deposits. During the lower Pliocene, drift aggradation increased and the drift migrated rapidly upslope forming an increasingly more pronounced moat (Fig. 4C). Influence of a downcutting current resulting in an increasing moat morphology has also been suggested by Reijmer *et al.* (2002). Since the upper Pliocene, the moat begins to act as a trap for mass flow deposits moving downslope (debrites and MTC) and prevents them from spreading into the basin (Fig. 4C). For very large mass transport complexes, the convex-up morphology of the drift acts as a decollement surface and allows the extension of deposits down to the basin (Principaud *et al.*, 2015).

Blake Plateau

The seismic units and unconformities observed on the Blake Plateau are partially consistent with those defined for the giant drift forming the Blake and Bahama Outer Ridge (Fig. 12; Benson *et al.*, 1978; Shipley *et al.*, 1978). The seismic units covering the Blake Plateau show well-stratified, layered, slightly undulated deposits with moderate seismic amplitude corresponding to a plastered drift geometry that covers a large surface of the plateau, sometimes forming a small detached drift when filling ancient slide scars (Fig. 12). The major drift bodies show downlap or onlap geometries defining major unconformities. The first unconformity is marked by a high-amplitude reflector located at the top of Unit 1 and is characterized by laminated continuous seismic facies (Fig. 12; Sheridan *et al.*, 1978). This unit is interpreted as the Jurassic–Cretaceous carbonate platform that was flooded during the Cenomanian sea-level rise. Consequently, this first unconformity corresponds to the A^u reflector (top Cenomanian; Benson *et al.*, 1978). The second unconformity (Merlin reflector) follows the top Cenomanian unconformity, in parts running parallel to it but also merging with it (Fig. 12) and is interpreted as the Eocene–Oligocene boundary (Sheridan *et al.*, 1979). The current that formed the latter is a deep current flowing at a water depth >2000 m. During the Eocene, the strength of the current along the sea floor at the Blake Plateau was not strong enough to erode the entire Eocene series as shown at the Blake and Bahama Outer Ridge (Fig. 12; Sheridan *et al.*, 1979). However, at places where the Eocene has been eroded, the sedimentary hiatus covers a period extending from the Cenomanian to the Eocene–Oligocene boundary, i.e. almost 60 Ma. A key point is the presence of folds affecting Unit 3. The folds are assumed to be related to a major folding period related to the growth of the Santaren Anticline during the Oligocene (Masaferro *et al.*, 2002). During this period, the feature illustrated in Fig. 12 would relate to large mass sliding over a detachment surface corresponding to the Eocene–Oligocene unconformity. The folds would thus correspond to compressional folds and the presence of extensional faults upslope is consistent with this interpretation. The unconformity forming the top of Unit 3 is proposed to be the top Oligocene unconformity as recognized on the Blake Bahama Outer Ridge (Sheridan *et al.*, 1979). The two upper discontinuities occurring in the upper part of the series can be correlated with those defined on the Blake and Bahama Outer Ridge, i.e. the late Miocene and late Pliocene unconformities, respectively (Fig. 12; Sheridan *et al.*, 1979). The eustatic lowstand in the early Miocene led to the combined intensification of the Gulf Stream in the study area and its shift to a more south-easterly location (Faugères & Stow, 2008). At present day the sea floor of the Blake Plateau lies between 1400 m and 1500 m water depth and during the Neogene the eustatic change did not exceed 150 m (Waelbroeck *et al.*, 2002). Hence, it seems unrealistic that the thick contourite deposits bounded by the unconformities are related to the activity of the warm, Gulf Stream surface current. As suggested by Faugères & Stow (2008), it is more likely that the most recent contourites (Pliocene and possibly early Pleistocene) that contributed to the formation of perched drifts on the Blake Plateau (Fig. 12) are related to the interaction of the Gulf Stream with the upper part of the Deep Western Boundary Current (DWBC) (Pinet & Popenoe, 1985). However, it seems that the most recent contourite accumulation occurs in slide scars or in small gateways allowing local current acceleration. The top of unit 6 shows mostly horizontal reflectors suggesting that the most recent deposition on the Blake Plateau is dominated by hemipelagites and that the Cenozoic contourite accumulation at this location is not currently active in the widespread flat areas forming the plateau. Results from Moal (2018) show that hemipelagite deposition has occurred at least since MIS 8. These hemipelagites are enriched in terrigenous clays during glacial periods either because of wind reinforcement or because of strengthening of the DWBC (Moal, 2018). Today the major unconformity acts as a decollement surface and gliding plane releasing large retrogressive planar slides towards the large Great Abaco Canyon (Mulder *et al.*, 2018a,b).

San Salvador Abyssal Plain

Deposition by contour currents is also evidenced in the deepest part of the system (Fig. 15). Core CI8108-13 shows clear alternations of white sediments with little grain-size variation (normal or reverse grading) and brown clay sediments with no grain-size variation (Fig. 15) consistent with observation of similar clay beds in other cores from the San Salvador area (Fig. 15; Cartwright, 1985). The Sr/Ca signal exhibits little variation, probably related to the important dissolution at this water depth (>4000 m) or little aragonite supply. The Al + K + Ti signal shows a clear correlation with the MIS chronology. This correlation is consistent with both intensified triggering of mass flow processes because of overloading related to higher production during interglacial periods with a large area of flooded platform (highstand shedding) and to intensified and thicker DWBC during glacial periods (Schmitt, 2013). The terrigenous input is clearly intensified during glacial stages. The analysis of several cores of the Bacar cruise (Schmitt, 2013) suggests that the carbonate particles forming the white layers are derived from the platform and are deposited through downslope carbonate gravity-flow processes. Conversely, brown layers would correspond to a supply by along-slope processes (fine-grained contourites). The clay deposited at this location most likely originated from the Irminger Basin (Greenland; Cartwright, 1985).

Accordingly, the mounded wedge-shaped structure observed along the Bahama Escarpment (Fig. 14) can be interpreted as a small detached drift built by the DWBC. The depression could be a small moat and/or a detachment surface related to the sliding of the contourite deposits along the Bahama Escarpment. Using this interpretation, the coarser wackestone layers observed in core CI8108-30 between 120 cm and 130 cm and between 490 cm and 510 cm could be reinterpreted as contourites rather than turbidites (Droxler, 1984; Cartwright, 1985).

Erosion by contour currents

Structures forming a negative topography observed on the Little Bahama Bank slope do not show evidence of flow directions (Fig. 5). The resolution of the backscatter image does not allow determination of whether they are either shallow erosional furrows or shallow depressions in between depositional patches. In both cases, they indicate either erosion of indurated substratum, or erosion of previously deposited soft sediment eroded by a stronger current. These erosional structures could be related to the Antilles Current down to 900 m water depth (Fig. 5A) but at greater water depths they probably are related to deeper currents forming the top of the North Atlantic Waters (DWBC; Fig. 5B; Meinen *et al.*, 2004). This would be consistent with the eastward bending of low-backscatter patches at the mouth of the canyons characterizing the slope of Little Bahama Bank (Fig. 5).

Along Great Bahama Bank, the sea floor at the moat shows scours and comet marks (Fig. 11). According to Werner *et al.* (1980) and Stow *et al.* (2009), giant comet marks result from erosion by energetic bottom currents, the scour length being relative to both the obstacle height and the current speed. This suggests the impact of a high-energy, north-pointing bottom current at this location (Grasmueck *et al.*, 2007; Correa *et al.*, 2012a,b). In the MTC area of Great Bahama Bank (Principaud *et al.*, 2015), the current direction is clearly indicated by the giant comet marks that occur downflow of the CWCM and blocks, a feature also observed by Lüdmann *et al.* (2016) (Fig. 11C). Tournadour (2015) interpreted the erosive furrows as the outcropping Pleistocene erosion surface. The bottom current cut the erosive furrows suggesting that current activity was high during the Holocene.

Along slope (contour currents) and downslope processes (gravity flows) interactions

The seismic section along the Great Bahama Bank slope (Fig. 4C) shows that the major contourite drift characterizing the basin floor contains gravity flow deposits that interfinger with the contourite deposits and are trapped and confined by the contouritic moat (Anselmetti *et al.*, 2000; Principaud *et al.*, 2015). At places, these gravity flow deposits partially or totally fill the moat (Rendle *et al.*, 2000; Principaud *et al.*, 2015; Schnyder *et al.*, 2016; Wunsch *et al.*, 2018). The Santaren Drift displays two distinct building phases (Langhian to Messinian and post-Pliocene) that are interrupted by toe of slope collapse events that occurred during the Pliocene and formed MTCs interbedded with the contourites (Fig. 4C; Anselmetti *et al.*, 2000; Principaud *et al.*, 2015). This sedimentation pattern suggests that gravity flows and contour currents are active at the same location, and that contour current deposits and gravity slope deposits interact continuously along the more than 270 km long slope of the western Great Bahama Bank. This interaction is active since the Langhian (Principaud *et al.*, 2018).

Low-backscatter patches at the mouth of the small canyons dissecting the Little Bahama Bank slope were interpreted as furrows formed in the distal part of the depositional system (Fig. 5). The eastward bending of these furrows indicates that the gravity flows at the origin of both canyons and downslope-elongated furrows are deflected by an eastward moving (along-slope) flow. This is consistent with the presence of along slope erosive lineaments cross-cutting the downslope-elongated structures (Fig. 5). It is proposed that the current flowing along the sea floor removed the finest carbonate particles transported by low-density turbidity currents flowing down the canyon axis. The removal of fine-grained particles would explain the cementation front as described by Tournadour (2015) for deposits occurring at *ca* 1100 m water depth. The increase in permeability of coarser grained sediments could favour increased cementation and enhanced diagenesis, a process that was also observed by Grammer *et al.* (1999). Finally, the current could also supply sufficient oxygen and nutrients to these surroundings enabling CWCM growth. The occurrence of pteropod beds in cores located in depressions of the lower Little Bahama Bank slope also suggests selective sediment concentration by currents (Chabaud, 2016; Chabaud *et al.*, 2016).

The most probable area with evidence of the interaction between contour-currents and downslope processes is the large submarine sedimentary system of the San Salvador Abyssal Plain (Fig. 13A). The carbonate turbidite system (Mulder *et al.*, 2018a,b) shows evidence for both downslope sedimentary processes and along-slope currents. The sediment waves with their crest perpendicular to the Samana Channel axis (sw1 and sw2 in Fig. 13B) and the furrows extending radially from the canyon mouth (f1 in Fig. 13B) have been interpreted as resulting from the spill-over of high energy turbidity currents along the left-hand side levée (Mulder *et al.*, 2018a,b). The features observed on the sea floor morphology include erosive north–south elongated furrows indicating the impact of an energetic north–south flowing current (f2 in Fig. 13B). The sediment waves with their crests oriented in an east–west direction can be interpreted as resulting from the same north–south current but with less energy (sw3 in Fig. 13B). The dissymmetry of the sediment waves suggests that the current is probably flowing southward (Fig. 13) that most likely is linked to the flow of DWBC water masses. The water depth is consistent with the DWBC activity along the Blake and Bahamas Outer Ridge but is deeper than the water depth measurements of Lee *et al.* (Fig. 3B; 1990). Cartwright (1985) also proposed that the sediment waves observed in the San Salvador area relate to the activity of DWBC and suggested that the presence of this energetic current resulted in an incomplete turbidite fan system and the presence of an important hiatus in the outer portion of the fan. The transition from furrows to sediment waves suggest a DWBC deceleration southward with the hypothesis that both furrows and waves have been formed in the same time period. The presence at this location of sedimentary features indicating both activity of downslope mass flow processes and along-slope currents suggests strongly that both processes could interact during some periods. In particular, the particles transported by the low velocity downslope processes can be pirated by the high-energy gravity flow and, conversely, particles carried further out by very low-energy downslope processes could be pirated by permanent contour currents at this location. Similar interactions between mass flow processes, in particular turbidity currents and contour currents (NADW) should similarly occur at a lesser scale at the mouth of Great Abaco Canyon and Little Abaco Canyon (GAC and LAC in Fig. 16).

Cold water carbonate mounds as indicators of contour currents

Lüdmann *et al.* (2016) demonstrated the link between the presence of cold water carbonate mounds (CWCM) and bottom currents (Antarctic Intermediate Water and Subtropical Underwater) in the Santaren Channel, between 285 m and 685 m water depth, off Cal Say Bank and Great Bahama Bank. The CWCM are preferentially developed in moats. Their location depends on the nutrient and oxygen supply by bottom currents (Neumann *et al.*, 1977; Mullins *et al.*, 1981). The CWCM localized on the middle slope of Little Bahama Bank correspond to true CWCM with living corals (type 1 of Lüdmann *et al.*, 2016) and consequently they are preferentially elongated in the downcurrent direction. They can be considered as active current markers and the main control parameters seem to be related to hydrodynamics, although the sedimentation rate, the nature of the substrate and the presence of fluids can also be control parameters (Neumann *et al.*, 1977; Mullins *et al.*, 1981; Messing *et al.*, 1990; Correa *et al.*, 2012a,b; Lüdmann *et al.*, 2016). Consequently, along-slope alignments of CWCM mark the trajectory of the Antilles Current along the middle slope of Little Bahama Bank and parabolic scours are developed in the downcurrent direction. These mounds also act as passive current markers. Similar structures are described by Wunsch *et al.* (2016) for the northern slopes of Cay Sal Bank where they are up to 700 m long and point south/south-west (Betzler *et al.*, 2014; Wunsch *et al.*, 2018).

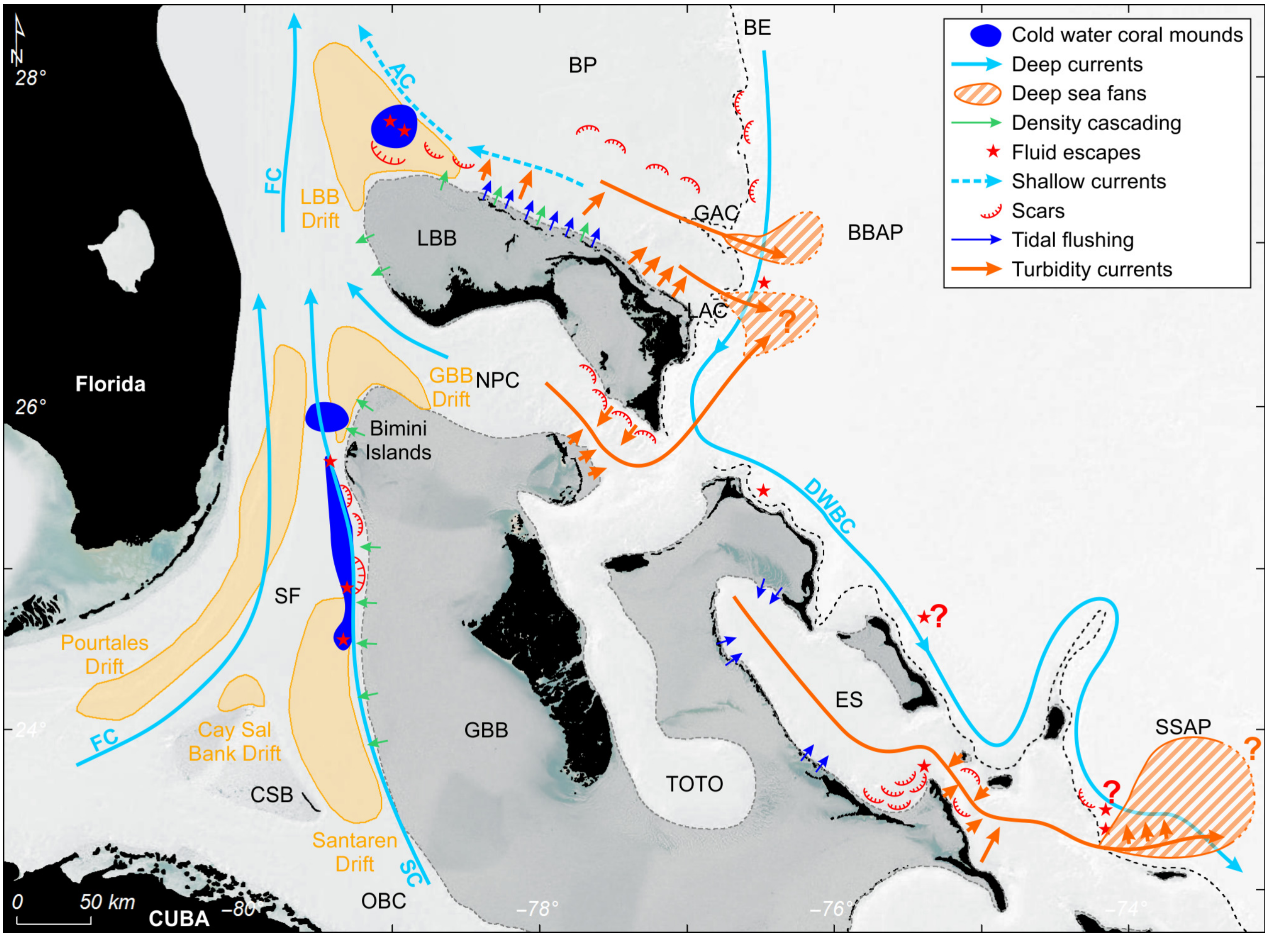

Fig. 16. Map of the Bahamas showing coverage of present-day knowledge of sediment transport and reworking including platform export (tidal flushing and density cascading), slope triggering (slides and mass transport complexes), downslope gravity flows (mainly turbidity currents) and contour currents related either to deep or shallow circulation. BBAP, Blake-Bahamas Abyssal Plain; BE, Bahama Escarpment; BP, Blake Plateau; CSB, Cay Sal Bank; ES, Exuma Sound; GAC, Great Abaco Canyon; GBB, Great Bahama Bank; LAC, Little Abaco Canyon; LBB, Little Bahama Bank; NPC, Northwest Providence Channel; OBC, Old Bahama Channel; SC, Santaren Channel; SF, Strait of Florida; SSAP, San Salvador Abyssal Plain; TOTO, Tongue of the Ocean.

At the western end of Little Bahama Bank, the rounded depressions observed are interpreted as pockmarks (Tournadour *et al.*, 2015). The topographic highs within these pockmarks are interpreted as CWCM and would correspond to the type 2 mounds of Lüdmann *et al.* (2016). They are not related to currents but rather to sub-bottom fluid escape. The fluid escape structures are associated with the large mass failure described by Tournadour (2015) and Tournadour *et al.* (2015) forming a large negative topography. This topography corresponds to the plane failure that followed the late Miocene unconformity and now is filled by sediments generating a layered echofacies interpreted as contourite deposits (Tournadour, 2015; Tournadour *et al.*, 2015). The type 3 mounds of Lüdmann *et al.* (2016) consist of blocks colonized by macro-epibenthos (for example, Gorgonia). These communities can sometimes transform to type 1 mounds of Lüdmann *et al.* (2016) when the summit becomes fully colonized by cold water corals. They are also underlined by crescent scours in the upstream direction and thus act also as passive current markers. The observed structures along the Great Bahama Bank slope (Fig. 11) resemble this type. The associated giant comet marks correspond to the scours described by Wunsch *et al.* (2016) and the parabolic scours of Lüdmann *et al.* (2016) from the upper slope of

Great Bahama Bank, and on the side of the Santaren Channel at *ca* 600 m water depth.

Sedimentary processes in the Bahamian archipelago

The Bahamas shows various sedimentary processes. Sediment is exported from the platform through tidal flushing (Fig. 16; Mulder *et al.*, 2017) or density cascading (Wilson & Roberts, 1995). It can directly form turbidity currents on steep slopes (Mulder *et al.*, 2018a,b) that may interact with contour currents. If deposited on slopes, sediment can be reactivated by mass failure and supply mass flow deposits that may interact with contour currents (Crevello & Schlager, 1980). Finally, contour currents can rework deposited deep sediment or winnow deposits and activate cementation; they also form erosional structures and deposits in particular when interacting with sea floor topography including CWCM.

CONCLUSIONS

The data collected during the Carambar cruises provided new insights into contourite depositional systems surrounding the Bahamian Archipelago. Structures observed on the present-day sea floor in seismic data indicate that the contour currents act at various water depths. The drifts surrounding the Bahamas are either related to surface currents or to deep bottom currents.

Sea-floor morphology has a strong impact on drift development. Little Bahama Bank and Great Bahama Bank drifts mainly develop following current expansion after passing the Strait of Florida and releasing sediment on the sides as well as sediments derived from the shallow parts of Little Bahama Bank and Great Bahama Bank.

The Bahamian slopes show a large variety of carbonate-dominated contourite drifts and contourite sequences. Only the deep-seated contour-current deposits located at the toe of the Bahama Escarpment have dominant siliciclastic content. The carbonate nature of the sediment, however, does not result in a drift morphology that is substantially different from those observed in siliciclastic or volcaniclastic sedimentary environments. Similar to what is observed in siliciclastic environments, carbonate drifts are essentially made up of fine-grained to very fine-grained material.

Major erosion surfaces recognized in other parts of the North Atlantic Ocean from the Langhian are also visible in the shallowest part of the Bahamian carbonate system (<1500 m water depth). These unconformities are particularly well-marked in the Straits of Florida and at the southern end of the Blake Plateau; they are related to changes in thermohaline circulation as a result of geodynamic, eustatic and climato-eustatic changes. These changes are related to the closure of the Central American Seaway and the formation of the Panama Isthmus that progressively occurred during middle and upper Miocene, between 15 Ma and 3·6 Ma. This major geodynamic change led to the establishment of present-day thermohaline circulation. Climato-eustatic changes were thus subordinate to these geodynamic changes and had a lesser but significant impact on contourite drift growth.

The deep-water current impact differs for the Santaren Drift where currents are situated at the toe of slope of Great Bahama Bank and a current is located at shallower locations; this determines the shape and position of the contourite drifts through time. The vertical evolution of the carbonate contourite sequence situated north-west of Little Bahama Bank shows a bi-gradational trend in grain-size related to a change in current velocity, similar to what is known from siliciclastic systems. However, carbonate contourite sequences are very condensed because of low sedimentation rates during glacial periods. The vertical nature of the contourite changes in relation to the source of the carbonate that depends strictly on variations in relative sea-level. During high sea-level, when the platform top is flooded, sediment supply is dominated by aragonite mud. With low sea-level exposing the platform top, the contourite is progressively enriched in planktonic foraminifera and pteropods, indicating that the major part of the biogenic fraction is produced in the open ocean water column. The contourite peak in grain size corresponds to an acceleration of the bottom currents, similar to what is observed for siliciclastic sediments, but is also associated with a decline in sediment supply in a carbonate system, whilst in siliciclastic systems it is frequently associated with higher sediment supply. The grain-size increase during the peak phase of the contour current is also related to increased winnowing that leads to cementation of the packstone facies.

Impact of hydrodynamics on cold water carbonate mound development seems to be important. The cold water carbonate mounds on Bahamian slopes develop either in current direction or on topographic highs to improve their nutrient and oxygen supply. That is an active interaction. In addition, cold water carbonate mounds also impact current hydrodynamics and locally generate erosion or induce deposition.

Downslope (mass flow) and along-slope (bottom current) processes are frequently active in the same area in the Bahamian system and can potentially interact. This leads to local enrichment of coarse material in contourites. Retroactively, drift growth can lead to confinement of gravity processes in contour current-related topographic lows (moats).

ACKNOWLEDGEMENTS

Authors thank the captain and crew of the *R/V L'Atalante* and the captain and crew of the *R/V Suroît* for the quality of the acquired data during the Carambar 1 and Carambar 2 cruises, respectively. Ifremer-Genavir is warmly thanked for cruise organization and technical support. This work has been supported by the French Institut National des Sciences de l'Univers program 'Actions Marges'. K. Fauquembergue, L. Chabaud, M. Principaud and E. Tournadour were funded by TOTAL. J.J.G. Reijmer thanks the College of Petroleum Engineering & Geosciences of KFUPM for their support (CPG – Carbonate Sedimentology Group publication no. 29). Authors acknowledge IHS for granting University of Bordeaux with academic Kingdom® software licences.

REFERENCES

Amos, A.F., **Gordon, A.L.** and **Schneider, E.D.** (1971) Water masses and circulation patterns in the region of the Blake-Bahama outer ridge. *Deep Sea Res. Oceanogr. Abstracts*, **18**, 145–165.

Anselmetti, F.S., **Eberli, G.P.** and **Ding, Z.-D.** (2000) From the Great Bahama Bank into the Straits of Florida: a margin architecture controlled by sea-level fluctuations and ocean currents. *Geol. Soc. Am. Bull.*, **112**, 829–844.

Atkinson, L.P., **Berger, T.**, **Hamilton, P.**, **Waddell, E.**, **Leaman, K.** and **Lee, T.N.** (1995) Current meter observations in the Old Bahama Channel. *J. Geophys. Res. Oceans*, **100**, 8555–8560.

Austin, J.A., **Schlager, W.**, **Palmer, A.A.**, **Comet, P.A.**, **Droxler, A.**, **Eberli, G.**, **Fourcade, E.**, **Freeman-Lynde, R.**, **Craig, S.**, **Fulthorpe, G.**, **Harwood, G.**, **Kuhn, D.**, **Lavoie, M.**, **Leckie, A.J.**, **Melillo, A.**, **Moore, H.T.**, **Mullins, C.**, **Ravenne, W.W.**, **Sager, P.**, **Swart, J.W.**, **Verbeek, D.K.**, **Watkins, , Williams, C.** (1986) *Proceedings ODP, Initial Report, Leg*, **101**. College Station, TX, 569 pp.

Austin, J.A., **Ewing, J.I.**, **Ladd, J.W.**, **Mullins, H.T.** and **Sheridan, R.E.** (1988) Seismic stratigraphic implications of ODP Leg 101 Site surveys. In: *Proceedings ODP, Scientific Research* (Eds J.A. Austin and W. Schlager *et al.*), **101**, 391–424.

Bein, A. and **Weiler, Y.** (1976) The Cretaceous Talme Yafe Formation: a contour current shaped sedimentary prism of calcareous detritus at the continental margin of the Arabian Craton. *Sedimentology*, **23**, 511–532.

Benson, W.E. and **Sheridan, R.E.**, **Pastouret, L.**, **Enos, P.**, **Freeman, T.**, **Murdmaa, I.O.**, **Worstell, P.**, **Gradstein, F.**, **Schmidt, R.R.**, **Weaver, F.M.**, **Stuermer, D.H.**, (1978) Initial reports of the Deep Sea Drilling Project, Vol. **44**. U.S. Government, Washington, D.C.

Bergman, K.L. (2005) Seismic analysis of paleocurrent features in the Florida Straits; insights into the paleo-Florida current, upstream tectonics, and the Atlantic-Caribbean connection. Unpublished PhD thesis, University of Miami, Coral Gables, FL, 206 pp.

Betzler, C., **Lindhorst, S.**, **Eberli, G.P.**, **Lüdmann, T.**, **Möbius, J.**, **Ludwig, J.**, **Schutter, I.**, **Wunsch, M.**, **Reijmer, J.J.G.** and **Hübscher, C.** (2014) Periplatform drift: the combined result of contour current and off-bank transport along carbonate platforms. *Geology*, **42**, 871–874.

Broecker, W.S. (1987) The biggest chill. *Nat. Hist. Mag.*, **97**, 74–82.

Brunner, C.A. (1975) Evidence for intensified bottom current activity in the Straits of Florida during the last glaciation. *Geol. Soc. Am.*, **7**, 1012–1013.

Brunner, C.A. (1986) Deposition of a muddy sediment drift in the southern Straits of Florida during the late Quaternary. *Mar. Geol.*, **69**, 235–249.

Cartwright, R.A. (1985) Provenance and sedimentology of carbonate turbidites from two deep-sea fans, Bahamas. Unpublished PhD thesis, University of Miami, Coral Gables, FL, 129 pp.

Chabaud, L. (2016) Modèle stratigraphique et processus sédimentaires au Quaternaire sur deux pentes carbonatées des Bahamas (leeward et windward). Unpublished PhD thesis, University of Bordeaux, Bordeaux, France, 419 pp.

Chabaud, L., **Ducassou, E.**, **Tournadour, E.**, **Mulder, T.**, **Reijmer, J.**, **Conesa, G.**, **Giraudeau, J.**, **Hanquiez, V.**, **Borgomano, J.** and **Ross, L.** (2016) Sedimentary processes determining the modern carbonate periplatform drift of Little Bahama Bank. *Mar. Geol.*, **318**, 213–229.

Chérubin, L.M. (2014) High-resolution simulation of the circulation in the Bahamas and Turks and Caicos Archipelagos. *Prog. Oceanogr.*, **127**, 21–46.

Coates, A.G., **Jackson, J.B.C.**, **Collins, L.S.**, **Cronin, T.M.**, **Dowsett, H.J.**, **Bybell, L.M.**, **Jung, P.** and **Obando, J.** (1992) Closure of the Isthmus of Panama: the near-shore marine record of Costa Rica and western Panama. *Geol. Soc. Am. Bull.*, **104**, 814–828.

Coates, A.G., **Collins, L.S.**, **Aubry, M.-P.** and **Berggren, W.A.** (2004) The Geology of the Darien, Panama, and the late Miocene-Pliocene collision of the Panama arc with northwestern South America. *Geol. Soc. Am. Bull.*, **116**, 1327–1344.

Cook, H.E. and **Mullins, H.T.** (1983) Basin margin environment. In: *Carbonate Depositional Environments* (Eds P.A. Scholle, D.G. Bebout and C.H. Moore), Am. Assoc. of Petrol. Geologists Memoir, **33**, 539–618.

Correa, T.B.S., **Eberli, G.P.**, **Grasmueck, M.**, **Reed, J.K.** and **Correa, A.M.S.** (2012a) Genesis and morphology of cold-water coral ridges in a unidirectional current regime. *Mar. Geol.*, **326–328**, 14–27.

Correa, T.B.S., **Grasmueck, M.**, **Eberli, G.P.**, **Reed, J.K.**, **Verwer, K.** and **Purkis, S.A.M.** (2012b) Variability of cold-water coral mounds in a high sediment input and tidal current regime, Straits of Florida. *Sedimentology*, **59**, 1278–1304.

Crevello, P.D. and **Schlager, W.** (1980) Carbonate debris sheets and turbidites, Exuma Sound, Bahamas. *J. Sed. Res.*, **50**, 1121–1147.

Croudace, I.W., **Rindby, A.** and **Rothwell, R.G.** (2006) ITRAX: description and evaluation of a new X-ray core scanner. In: *New Ways of Looking at Sediment Cores and Core Data* (Ed. R.G. Rothwell), Geological Society Special Publication, **267**, 51–63.

Droxler, A.W. (1984) Late Quaternary glacial cycles in the Bahamian deep basins and in the adjacent Atlantic Ocean. Unpublished PhD thesis, University of Miami, Coral Gables, FL, 165 pp.

Eberli, G.P. and **Betzler, C.** (2019) Characteristics of modern carbonate contourite drifts. *Sedimentology*, **66**, 1163–1191.

Eberli, G.P. and **Ginsburg, R.N.** (1989). Cenozoic progradation of northwestern Great Bahama Bank, a record of lateral platform growth and sea-level fluctuations. In: *Controls on Carbonate Platform and Basin Systems* (Eds P.D. Crevello, J.A. Wilson, J.F. Read and F.J. Sarg), SEPM Special Publication, **44**, 339–351.

Eberli, G.P., **Swart, P.K.**, **Malone, M.J.**, **Anselmetti, F.S.**, **Arai, K.**, **Bernet, K.H.**, **Betzler, C.**, **Christensen, B.A.**, **De Carlo, E.H.**, **Déjardin, P.M.**, **Emmanuel, L.**, **Frank, T.D.**, **Haddad, G.A.**, **Isern, A.R.**, **Katz, M.E.**, **Kenter, J.A.M.**, **Kramer, P.A.**, **Kroon, D.**, **McKenzie, J.A.**, **McNeill, D.F.**, **Montgomery, P.**, **Nagihara, S.**, **Pirmez, Ca.**, **Reijmer, J.J.G.**, **Sato, T.**, **Schovsbo, N.H.**, **Williams, T.** and **Wright, J.D.**, (1997a) *Proceedings ODP, Initial Report*, **166**, College Station, Texas, 850 pp.

Eberli, G.P., **Swart, P.K.**, **McNeill, D.F.**, **Kenter, J.A.M.**, **Anselmetti, F.S.**, **Melim, L.A.** and **Ginsburg, R.N.** (1997b) A synopsis of the Bahamas Drilling Project: results from two deep core borings drilled on the Great Bahama Bank. In: *Proceedings ODP, Initial Report* (Eds G.P. Eberli, P.K. Swart and M.J. Malone *et al.*), **166**, 23–41.

Evans, H.K., **Hall, I.R.**, **Bianchi, G.G.** and **Oppo, D.W.** (2007) Intermediate water links to Deep Western Boundary current variability in the subtropical NW Atlantic during Marine Isotope stages 5 and 4. *Paleoceanography*, **22**, PA3209. https://doi.org/10.1029/2006pa001409

Ewing, J.I. and **Hollister, C.D.** (1972) Regional aspects of deep sea drilling in the western North Atlantic. In: *Initial Reports of the Deep Sea Drilling Project*, Vol. XI (Eds C.D. Hollister *et al.*), pp. 951–973. U.S. Govt. Printing Office, Washington, D.C.

Faugères, J.-C. and **Mulder, T.** (2010) Contour currents and contourite drifts, In: *Deep-Sea Sediments* (Eds. H. Hüneke and T. Mulder), Developments in Sedimentology, Elsevier, **63**, 149–214.

Faugères, J.-C. and **Stow, D.A.V.** (2008) Contourite drifts: nature, evolution and controls. In: *Contourites* (Eds M. Rebesco and A. Camerlenghi), Developments in Sedimentology, **60**, 259–288.

Faugères, J.-C., **Gonthier, E.** and **Stow, D.A.V.** (1984) Contourite drift molded by deep Mediterranean outflow. *Geology*, **12**, 296–300.

Faugères, J.-C., **Stow, D.A.V.**, **Imbert, P.** and **Viana, A.** (1999) Seismic features diagnostic of contourite drifts. *Mar. Geol.*, **162**, 1–38.

Fauquembergue, K., **Ducassou, E.**, **Mulder, T.**, **Hanquiez, V.**, **Perello, M.-C.**, **Poli, E.** and **Borgomano, J.** (2018) Genesis and growth of a carbonate Holocene wedge on the Northern Little Bahama Bank. *Mar. Petrol. Geol.*, **96**, 602–614.

Gonthier, E.G., **Faugères, J.-C.** and **Stow, D.A.V.** (1984) Contourite facies of the Faro Drift, Gulf of Cadiz. *Geol. Soc. London. Spec. Publ.*, **15**, 275–292.

Grammer, G.M. and **Ginsburg, R.N.** (1992) Highstand versus lowstand deposition on carbonate platform margins: insight from Quaternary foreslopes in the Bahamas. *Mar. Geol.*, **103**, 125–136.

Grammer, G.M., **Ginsburg, R.N.** and **Harris, P.M.** (1993) Timing of deposition, diagenesis, and failure of steep carbonate slopes in response to a high-amplitude/high frequency fluctuation in sea level, tongue of the ocean, Bahamas. In: *Carbonate Sequence Stratigraphy: Recent Developments and Applications* (Eds R.G. Loucks and J.F. Sarg), pp. 107–131. American Association of Petroleum Geologists, Tulsa, OK.

Grammer, G.M., **Crescini, C.M.**, **McNeill, D.F.** and **Taylor, L.H.** (1999) Quantifying rates of syndepositional marine cementation in deeper platform environments—new insight into a fundamental process. *J. Sed. Res.*, **69**, 202–207.

Grasmueck, M., **Eberli, G.P.**, **Viggiano, D.A.**, **Correa, T.**, **Rathwell, G.** and **Luo, J.** (2006) Autonomous underwater vehicle (AUV) mapping reveals coral mound distribution, morphology, and oceanography in deep water of the Straits of Florida. *Geophys. Res. Lett.*, **33**, L23616. https://doi.org/10.1029/2006GL027734.

Grasmueck, M., **Eberli, G.**, **Correa, T.B.S.**, **Viggiano, D.A.**, **Luo, J.**, **Wyatt, G.J.**, **Reed, J.K.**, **Wright, A.E.** and **Pomponi, S.A.** (2007) AUV-based environmental characterization of deep-water coral mounds in the Straits of Florida. *Offshore Technology Conference, Houston, Texas*, pp. 1–11.

Haq, B.U., **Hardenbol, J.** and **Vail, P.R.** (1987) Chronology of fluctuating sea levels since the Triassic. *Science*, **235**, 1156–1167.

Haug, G.H. and **Tiedemann, R.** (1998) Effect of the formation of the Isthmus of Panama on Atlantic Ocean thermohaline circulation. *Nature*, **393**, 673–676.

Heezen, B.C. and **Hollister, C.D.** (1971) *The Face of the Deep.* Oxford University Press, London, 659 pp.

Howe, J.A., **Stoker, M.S.** and **Stow, D.A.V.** (1994) Late Cenozoic sediment drift complex, northeast Rockall Trough, North Atlantic. *Paleoceanography*, **9**, 989–999.

Hüneke, H. and **Stow, D.A.V.** (2008) Identification of ancient contourites: problems and paleoceanographic significance. In: *Contourites* (Eds M. Rebesco and A. Camerlenghi). Development in Sedimentology, **60**, 323–344.

Johns, W.E., **Shay, T.J.**, **Bane, J.M.** and **Watts, D.R.** (1995) Gulf Stream structure, transport and recirculation near 68W. *J. Geophys. Res.*, **100**, 817–838.

Kullenberg, B. (1947) The piston core sampler. *SvensJca HydrografisJc-Biologiska Rommissionens skrifter. Tredje Serien: Hydrografl*, **1**, 1–46.

Lantzsch, H., **Roth, S.**, **Reijmer, J.J.G.** and **Kinkel, H.** (2007) Sea-level related resedimentation processes on the northern slope of Little Bahama Bank (Middle Pleistocene to Holocene). *Sedimentology*, **54**, 1307–1322.

Leaman, K.D., **Vertes, P.S.**, **Atkinson, L.P.**, **Lee, T.N.**, **Hamilton, P.** and **Waddell, E.** (1995) Transport, potential vorticity, and current/temperature structure across Northwest Providence and Santaren Channels and the Florida Current off Cay Sal Bank. *J. Geophys. Res.*, **100**, 8561–8569.

Lee, T.N., **Johns, W.E.**, **Zantopp, R.** and **Schott, F.** (1990) Western boundary current structure and variability east of Abaco, Bahamas at 26.5°N. *J. Phys. Oceanogr.*, **20**, 446–466.

Locker, S.D. and **Laine, P.** (1992) Paleogene-Neogene depositional history of the middle U.S. Atlantic continental rise: mixed turbidite and contourite depositional systems. *Mar. Geol.*, **103**, 137–164.

Lüdmann, T., **Kalvelage, C.**, **Betzler, C.**, **Fürstenau, J.** and **Hübscher, C.** (2013) The Maldives, a giant isolated carbonate platform dominated by bottom currents. *Mar. Petrol. Geol.*, **43**, 326–340.

Lüdmann, T., **Paulat, M.**, **Betzler, C.**, **Mobius, J.**, **Lindhorst, S.**, **Wunsch, M.** and **Eberli, G.P.** (2016) Carbonate mounds in the Santaren Channel, Bahamas: a current-dominated periplatform depositional regime. *Mar. Geol.*, **376**, 69–85.

Lüdmann, T., **Betzler, C.**, **Eberli, G.P.**, **Reolid, J.**, **Reijmer, J.J.G.**, **Sloss, C.R.**, **Bialik, O.M.**, **Alvarez-Zarikian, C.A.**, **Alonso-García, M.**, **Blättler, C.L.**, **Guo, J.A.**, **Haffen, S.**, **Horozal, S.**, **Inoue, M.**, **Jovane, L.**, **Kroon, D.**, **Lanci, L.**, **Laya, J.C.**, **Mee, A.L.H.**, **Nakakuni, M.**, **Nath, B.N.**, **Niino, K.**, **Petruny, L.M.**, **Pratiwi, S.D.**, **Slagle, A.L.**, **Su, X.**, **Swart, P.K.**, **Wright, J.D.**, **Yao, Z.** and **Young, J.R.** (2018) Carbonate delta drift: a new sediment drift type. *Mar. Geol.*, **401**, 98–111.

Masaferro, J.L., **Bulnes, M.**, **Poblet, J.** and **Eberli, G.P.** (2002) Episodic folding inferred from syntectonic carbonate sedimentation: the Santaren Anticline, Bahamas Foreland. *Sed. Geol.*, **146**, 11–24.

McCave, I.N. and **Carter, L.** (1997) Recent sedimentation beneath the Deep Western Boundary Current off northern New Zealand. *Deep Sea Res. Part I Oceanogr. Res. Pap.*, **44**, 1203–1237.

McCave, I.N. and **Tucholke, B.E.** (1986) Deep current-controlled sedimentation in the western North Atlantic. In: *The Western North Atlantic Region* (Eds P.R. Vogt and B.E. Tucholke), pp. 451–468. The Geological Society of America, Boulder, Colorado.

McMaster, R.L., **Locker, S.D.** and **Laine, E.P.** (1989) The early Neogene continental rise off the eastern United States. *Mar. Geol.*, **87**, 137–163.

Meinen, C.S., **Garzoli, S.L.**, **Johns, W.E.** and **Baringer, M.O.** (2004) Transport variability of the Deep Western Boundary Current and the Antilles Current off Abaco Island, Bahamas. *Deep Sea Res. Part I Oceanogr. Res. Pap.*, **51**, 1397–1415.

Messing, C.G., **Neumann, A.C.** and **Lang, J.C.** (1990) Biozonation of deep-water lithoherms and associated hardgrounds in the northeastern Straits of Florida. *Palaios*, **5**, 15–33.

Meyerhoff, A.A. and **Hatten, C.W.** (1974) Bahamas salient of North America: tectonic framework, stratigraphy, and petroleum potential. *AAPG Bull.*, **58**, 1201–1239.

Moal, P. (2018) Marge nord de Gerat Abaco Canyon: analyses stratigraphiques et sédimentologiques. Unpublished MSc thesis, University of Bordeaux, Bordeaux, France, 36 pp.

Mountain, G.S. and **Tucholke, B.E.** (1985) Mesozoic and Cenozoic geology of the U.S. Atlantic continental slope and rise. In: *Geologic Evolution of the United States Atlantic Margin* (Ed. C.W. Poag), pp. 293–341. Van Nostrand Reinhold Company Inc, New York.

Mulder, T., **Ducassou, E.**, **Gillet, H.**, **Hanquiez, V.**, **Tournadour, E.**, **Combes, J.**, **Eberli, G.P.**, **Kindler, P.**, **Gonthier, E.**, **Conesa, G.**, **Robin, C.**, **Sianipar, R.**, **Reijmer, J.J.G.** and **François, A.** (2012a) Canyon morphology on a modern carbonate slope of the Bahamas: evidence of regional tectonic tilting. *Geology*, **40**, 771–774.

Mulder, T., **Ducassou, E.**, **Hanquiez, V.**, **Gonthier, E.**, **Kindler, P.**, **Principaud, M.**, **Fournier, F.**, **Léonide, P.**, **Billeaud, I.**, **Marsset, B.**, **Reijmer, J.J.G.**, **Bondu, C.**, **Joussiaume, R.** and **Pakiades, M.** (2012b) New insights into the morphology and sedimentary processes along the western slope of Great Bahama Bank. *Geology*, **40**, 603–606.

Mulder, T., **Jumes, M.**, **Hanquiez, V.**, **Gillet, H.**, **Reijmer, J.J.G.**, **Tournadour, E.**, **Chabaud, L.**, **Principaud, M.**, **Schnyder, J.**, **Borgomano, J.**, **Fauquembergue, K.**, **Ducassou, E.** and **Busson, J.** (2017) Carbonate slope morphology revealing sediment transfer from bank-to-slope (Little Bahama Bank, Bahamas). *Marine Petroleum Geol.*, **83**, 26–34.

Mulder, T., **Gillet, H.**, **Hanquiez, V.**, **Ducassou, E.**, **Fauquembergue, K.**, **Principaud, M.**, **Conesa, G.**, **Le Goff, J.**, **Ragusa, J.**, **Bashah, S.**, **Bujan, S.**, **Reijmer, J.J.G.**, **Cavailhes, T.**, **Droxler, A.W.**, **Blank, D.G.**, **Guiastrennec, L.**, **Fabregas, N.**, **Recouvreur, A.** and **Seibert, C.** (2018a) Carbonate slope morphology revealing a giant submarine canyon (Little Bahama Bank, Bahamas). *Geology*, **46**, 31–34.

Mulder, T., **Gillet, H.**, **Hanquiez, V.**, **Reijmer, J.J.G.**, **Droxler, A.W.**, **Recouvreur, A.**, **Fabregas, N.**, **Cavailhes, T.**, **Fauquembergue, K.**, **Blank, D.G.**, **Guiastrennec, L.**, **Seibert, C.**, **Bashah, S.**, **Bujan, S.**, **Ducassou, E.**, **Principaud, M.**, **Conesa, G.**, **Le Goff, J.**, **Ragusa, J.**, **Busson, J.** and **Borgomano, J.** (2018b) Into the deep: a coarse-grained carbonate turbidite valley and canyon in ultra-deep carbonate setting. *Mar. Geol.*, **407**, 316–333.

Mullins, H.T. and **Neumann, A.C.** (1979) Deep carbonate bank margin structure and sedimentation in the Northern Bahamas. *SEPM Spec. Pub.*, **27**, 165–192.

Mullins, H.T., **Neumann, A.C.**, **Wilber, R.J.**, **Hine, A.C.** and **Chingurg, S.J.** (1980) Carbonate sediment drifts in northern Straits of Florida. *AAPG Bull.*, **64**, 1701–1717.

Mullins, H.T., **Newton, C.R.**, **Heath, K.** and **Van Buren, H.M.** (1981) Modern deep-water coral mounds north of Little Bahama Bank; criteria for recognition of deep-water coral bioherms in the rock record. *J. Sed. Res.*, **51**, 999–1013.

Mullins, H.T., **Heath, K.C.**, **Van Buren, H.M.** and **Newton, C.R.** (1984) Anatomy of a modern open-ocean carbonate slope: northern Little Bahama Bank. *Sedimentology*, **31**, 141–168.

Mullins, H.T., **Gardulski, A.F.**, **Wise, S.W.** and **Applegate, J.** (1987) Middle Miocene oceanographic event in the eastern Gulf of Mexico: implications for seismic stratigraphic succession and Loop Current/Gulf Stream circulation. *Geol. Soc. Am. Bull.*, **98**, 702–713.

Neumann, A.C. and **Ball, M.M.** (1970) Submersible observations in the Straits of Florida: geology and bottom currents. *Geol. Soc. Am. Bull.*, **81**, 2861–2874.

Neumann, G. and **Pierson, W.J.** (1966) *Principles of Physical Oceanography*. Prentice Hall, Englewood Cliffs, NJ, 545 pp.

Neumann, A.C., **Kofoed, J.W.** and **Keller, G.H.** (1977) Lithoherms in the Straits of Florida. *Geology*, **5**, 4–10.

Paulat, M., **Lüdmann, T.**, **Betzler, C.** and **Eberli, G.P.** (2019) Neogene palaeoceanographic changes recorded in a carbonate contourite drift (Santaren Channel, Bahamas). *Sedimentology*, **66**, 1361–1385.

Pindell, J.L. (1994) Chapter 2: Evolution of the Gulf of Mexico and the Caribbean. In: *Caribbean Geology: An Introduction* (Eds S.K. Donovan and T.A. Jackson), pp. 13–39. U.W.I. Publ. Ass., Kingston.

Pinet, P.R. and **Popenoe, P.** (1985) A scenario of Mesozoic-Cenozoic ocean circulation over the Blake Plateau and its environs. *Geol. Soc. Am. Bull.*, **96**, 618–626.

Principaud, M. (2015) Morphologie, architecture et dynamique sédimentaire d'une pente carbonatée moderne, le Great Bahama Bank (Bahamas). Unpublished PhD. Thesis, University of Bordeaux, Bordeaux, France, 293 pp.

Principaud, M., **Mulder, T.**, **Gillet, H.** and **Borgomano, J.** (2015) Large-scale carbonate mass-wasting along the Northwestern slope of the Great Bahama Bank (Bahamas): morphology, architecture, and mechanisms. In: *Carbonate Slopes and Gravity Deposits* (Eds T. Mulder, J.J.G. Reijmer and J. Borgomano), Sed. Geol., Spec. Issue, **317**, 27–42.

Principaud, M., **Ponte, J.-P.**, **Mulder, T.**, **Gillet, H.**, **Robin, C.** and **Borgomano, J.** (2018) Slope-to-basin stratigraphic evolution of the carbonate northwestern Great Bahama Bank (Bahamas) during the Neogene-Quaternary: interactions between downslope and bottom currents deposits. *Basin Res.*, **29**, 699–724.

Rebesco, M. (2005) Contourites. In: *Encyclopedia of Geology* (Eds R.C. Selley, L.R.M. Cocks and I.R. Plimer), pp. 513–527. Elsevier, Oxford.

Rebesco, M., **Camerlenghi, A.** and **Van Loon, A.J.** (2008) Contourite research: a field in full development. In: *Contourites* (Eds M. Rebesco and A. Camerlenghi). Developments in Sedimentology, **60**, 3–10.

Rebesco, M., **Hernández-Molina, F.J.**, **Van Rooij, D.** and **Wählin, A.** (2014) Contourites and associated sediments controlled by deep-water circulation processes: state of the art and future considerations. *Mar. Geol.*, **352**, 111–154.

Reeder, M.S., **Rothwell, G.** and **Stow, D.A.V.** (2002) The Sicilian gateway: anatomy of the deepwater connection between East and West Mediterranean basins. In: *Deep-water Contourite Systems: Modern Drifts and Ancient Series, Seismic and Sedimentary Characteristics* (Eds D.A.V. Stow, C.J. Pudsey, J.A. Howe, J.-C. Faugères and A.R. Viana), Geol. Soc. London, **22**, 171–189.

Reijmer, J.J.G., **Betzler, C.**, **Kroon, D.**, **Tiedemann, R.** and **Eberli, G.** (2002) Bahamian carbonate platform development in response to sea-level changes and the closure of the Isthmus of Panama. *Int. J. Earth Sci.*, **91**, 482–489.

Rendle, R.H., **Reijmer, J.J.G.**, **Kroon, D.** and **Henderson, G.M.** (2000) Mineralogy and sedimentology of the Pleistocene to Holocene on the leeward margin of Great Bahama Bank. In: *Proceedings of the Ocean Drilling Program, Scientific Results Leg 166* (Eds P.K. Swart, G.P. Eberli, P.K. Swart, M.J. Malone and J.F. Sarg). pp. 61–76. Ocean Drilling Program, College Station, TX.

Rendle-Bühring, R.H. and **Reijmer, J.J.G.** (2005) Controls on grain-size patterns in periplatform carbonates: marginal setting versus glacio-eustacy. *Sed. Geol.*, **175**, 99–113.

Richardson, W.S., **Schmitz, W.J.** and **Niiler, P.P.** (1969) The velocity structure of the Florida Current from the Straits of Florida to Cape Fear. *Deep-Sea Res.*, **Suppl 16**, 225–231.

Schlager, W. and **Chermak, A.** (1979) Sediment facies of platform basin -transition, Tongue of the Ocean, Bahamas. In: *Geology of Continental Slopes* (Eds L.J. Doyle and O.H. Pilkey), Society of Economic Paleontologists and Mineralogists Spec. Publ., **27**, 193–207.

Schlager, W., **Austin, J.A.**, **Corso, W.**, **McNulty, C.L.**, **Fluegel, E.**, **Renz, O.** and **Steinmetz, J.C.** (1984) Early Cretaceous platform re-entrant and escarpment erosion in the Bahamas. *Geology*, **12**, 147–150.

Schlager, W., **Bourgeois, F.**, **Mackenzie, G.** and **Smit, J.** (1988) Boreholes at great isaac and site 626 and the history of the Florida Straits. In: *Proceeding of the Ocean Drilling Program, Scientific Results* (Eds J.A. Austin, W. Schlager, *et al.*), Ocean Drilling Program: College Station, TX, **101**, 425–437.

Schmitt, A. (2013) Etudes des processus de dépôt des marges carbonatées dans les Bahamas: Exemple du Petit Banc des Bahamas et de San Salvador. Unpublished MSc thesis, University of Bordeaux, Bordeaux, France, 48 pp.

Schmitz, W.J. and **Richardson, W.S.** (1991) On the sources of the Florida Current. *Deep-Sea Res.*, **30**, no. Supplemental 1, S379–S409.

Schnyder, J., **Eberli, G.P.**, **Kirby, J.**, **Shi, F.**, **Tehranirad, B.**, **Mulder, T.**, **Ducassou, E.**, **Hebbeln, D.** and **Wintersteller, P.** (2016) Tsunamis caused by submarine slope failures along western Great Bahama Bank. *Nat. Sci. Rep.*, **6**, 35925. https://doi.org/10.1038/srep35925.

Shanmugam, G. (2006) *Deep-water Processes and Facies Models. Implications for Sandstone Petroleum Reservoirs. Handbook of Petroleum Exploration and Production 5*. Elsevier, Amsterdam, 476 pp.

Shanmugam, G. (2008) Deep-water bottom currents and their deposits. In: *Contourites* (Eds M. Rebesco and A. Camerlenghi). Development in Sedimentology, **60**, 289–300.

Sheridan, R.E., **Pastouret, L.** and **Mosditchian, G.** (1978) Seismic stratigraphy and related lithofacies of the Blake-Bahama Basin. In: *Initial reports of the Deep Sea Drilling Project*, Vol. **44** (Eds W.E. Benson and R.E. Sheridan, *et al.*), pp. 529–554. U.S. Government Printing Office, Washington, D.C.

Sheridan, R.E., **Windisch, C.C.**, **Ewing, J.I.** and **Stoffa, P.L.** (1979) Structure and stratigraphy of the Blake Escarpment based on seismic reflection profiles. In: *Geological and Geophysical Investigations of Continental Margins* (Eds J.S. Watkins, L. Montadert and P.W. Dickerson), American Association of Petroleum Geologists Memoir, **29**, 77–186.

Sheridan, R., **Gradstein, F.**, **Barnard, L.A.**, **Bliefnick, D.M.**, **Habib, D.**, **Jenden, P.D.**, **Kagami, H.**, **Keenan, E.M.**, **Kostecki, J.**, **Kvenvolden, K.**, **Moullade, M.**, **Ogg, J.A.**, **Robertson, A.H.F.**, **Roth, P.H.** and **Shipley, T.** (1983) Site 533: blake outer ridge. In: *Initial Reports Deep Sea Drilling Project (DSDP) 76* (Eds. R.E. Sheridan, F.M. Gradstein, *et al.*), pp. 35–139. U.S. Govt. Printing Office, Washington.

Sheridan, R.E., **Mullins, H.T.**, **Austin, J.J.A.**, **Ball, M.M.** and **Ladd, J.W.** (1988) Geology and geophysics of the Bahamas. In: *Geology of North America* (Eds R.E. Sheridan and J.A. Grow), The Atlantic Continental Margin. Geological Society of America, **1–2**, 177–196.

Shipley, T.H., **Buffler, R.T.** and **Watkins, J.S.** (1978) Seismic stratigraphy and geologic history of Blake Plateau and adjacent western Atlantic continental margin. *AAPG Bull.*, **62**, 792–812.

Steph, S., **Tiedemann, R.**, **Prange, M.**, **Groeneveld, J.**, **Nürnberg, D.**, **Reuning, L.**, **Schulz, M.** and **Haug, G.H.**

(2006) Changes in Caribbean surface hydrography during the Pliocene shoaling of the Central American Seaway. *Paleoceanography*, **21**, 1–25.

Stow, D.A.V. (1994) Deep-sea processes of sediment transport and deposition. In: *Sediment Transport and Depositional Processes*(Ed. K. Pye), pp. 257–291. Blackwell, Oxford.

Stow, D.A.V., **Reading, H.G.** and **Collinson, J.** (1996) Chapter 10. Deep seas. In: *Sedimentary Environments: Processes, Facies and Stratigraphy* (Ed. H.G. Reading), pp. 395–453. Wiley-Blackwell, Oxford.

Stow, D.A.V., **Faugères, J.-C.**, **Howe, J.**, **Pudsey, C.J.** and **Viana, A.R.** (2002a) Bottom currents, contourites and deep-sea sediment drifts: current state-of-art. In: *Deep-Water Contourites: Modern Drifts and Ancient Series, Seismic and Sedimentary Characteristics* (Eds D.A.V. Stow, C.J. Pudsey, J.A. Howe, J.-C. Faugères and A.R. Viana), Geol. Soc. London, Mem., **22**, 7–20.

Stow, D.A.V., **Faugères, J.-C.**, **Gonthier, E.**, **Cremer, M.**, **Llave, E.**, **Hernandez-Molina, F.J.**, **Somoza, L.** and **Diaz-Del-Rio, V.** (2002b). Faro-Albufeira drift complex, northern Gulf of Cadiz. In: *Deep-Water Contourite Systems: Modern Drifts and Ancient Series, Seismic and sedimentary Characteristics* (Eds D.A.V. Stow, C.J. Pudsey, J.A. Howe, J.-C. Faugères and A.R. Viana). Geol. Soc. London Mem., 137–154.

Stow, D.A.V., **Hunter, S.**, **Wilkinson, D.** and **Hernández-Molina, F.J.** (2008). The nature of contourite deposition. In: *Contourites* (Eds M. Rebesco and A. Camerlenghi). Developments in Sedimentology, **60**, 143–156.

Stow, D.A.V., **Hernández-Molina, F.J.**, **Llave, E.**, **Sayazo-Gil, M.**, **Dıáz del Río, V.** and **Branson, A.** (2009) Bedform-velocity matrix: the estimation of bottom-current velocity from bedform observations. *Geology*, **37**, 327–330.

Tournadour, E. (2015) Architecture et dynamique sédimentaire d'une pente carbonatée moderne: exemple de la pente Nord de Little Bahama Bank (LBB), Bahamas. Unpublished PhD thesis, University of Bordeaux, Bordeaux, France, 323 pp.

Tournadour, E., **Mulder, T.**, **Borgomano, J.**, **Hanquiez, V.**, **Ducassou, E.** and **Gillet, H.** (2015) Origin and architecture of a Mass Transport Complex on the northwest slope of Little Bahama Bank (Bahamas): relations between off-bank transport, bottom current sedimentation and submarine landslides. *Sed. Geol.*, **317**, 9–26.

Tucholke, B.E. (2002) The Greater Antilles Outer Ridge: development of a distal sedimentary drift by deposition of fine-grained contourites. In: *Deep-Water Contourite Systems: Modern Drifts and Ancient Series, Seismic and Sedimentary Characteristics* (Eds D.A.V. Stow, C.J. Pudsey, J.A. Howe, J.-C. Faugères and A.R. Viana). Geol. Soc. London Mem., **22**, 39–55.

Tucholke, B.E. and **Mountain, G.S.** (1979) Seismic stratigraphy, lithostratigraphy, and paleosedimentation patterns in the North American Basin. *Am. Geophys. Union Maurice Ewing Ser.*, **3**, 58–86.

Tucholke, B.E. and **Mountain, G.S.** (1986) Tertiary paleoceanography of the western North Atlantic Ocean. In: *The Geology of North America, Volume M, The Western North Atlantic Region* (Eds P.R. Vogt and B.E. Tucholke), pp. 631–650. Geol. Soc. Am., Boulder, CO.

Viana, A.R., **Faugères, J.-C.** and **Stow, D.A.V.** (1998) Bottom-current-controlled sand deposits – a review of modern shallow- to deep-water environments. *Sed. Geol.*, **115**, 53–80.

Waelbroeck, C., **Labeyrie, L.**, **Michel, E.**, **Duplessy, J.-C.**, **McManus, J.F.**, **Lambeck, K.**, **Balbon, E.** and **Labracherie, M.** (2002) Sea-level and deep water temperature changes derived from benthic foraminifera isotopic records. *Quatern. Sci. Rev.*, **21**, 295–305.

Wang, J. and **Mooers, C.N.K.** (1997) Three-dimensional perspective of the Florida Current: transport potential vorticity, and related dynamical properties. *Dynam. Atmos. Oceans*, **27**, 135–149.

Werner, F., **Unsold, G.**, **Koopmann, B.** and **Stefanon, A.** (1980) Field observations and flume experiments on the nature of comet marks. *Sed. Geol.*, **26**, 233–262.

Wilson, P.A. and **Roberts, H.H.** (1995) Density cascading: off-shelf sediment transport, evidence and implications, Bahama Banks. *J. Sediment. Res.*, **A65**, 45–56.

Wunsch, M., **Betzler, C.**, **Lindhorst, S.**, **Lüdmann, T.** and **Eberli, G.P.** (2016) Sedimentary dynamics along carbonate slopes (Bahamas archipelago). *Sedimentology*, **64**, 631–657.

Wunsch, M., **Betzler, C.**, **Eberli, G.P.**, **Lindhorst, S.**, **Lüdmann, T.** and **Reijmer, J.J.G.** (2018) Sedimentary dynamics and high-frequency sequence stratigraphy of the southwestern slope of Great Bahama Bank. *Sed. Geol.*, **363**, 96–117.

Wynn, R.B. and **Masson, D.G.** (2008). Sediment waves and bedforms. In: *Contourites* (Eds M. Rebesco and A. Camerlenghi). Developments in Sedimentology, **60**, 289–300.

Manuscript received 17 April 2018; revision accepted 30 January 2019